Techno-Economic Analysis of Cyclic Carbonate Synthesis

Research Project

Kees Elstgeest S5317460

March 4, 2025

1 Abstract

This study investigates the sustainable synthesis of cyclic carbonates via the cycloaddition reaction of CO_2 to epoxides, aiming to transform a greenhouse gas into high-value chemicals with applications in polymer production, solvents, and energy storage. Three substrates, allyl glycidyl ether, butylene oxide, and glycidol, were evaluated under similar reaction conditions using an ion-exchanged Merrifield resin catalyst (Amberlite IRA-910). The process was first optimized in a 100 mL batch reactor and subsequently scaled to a 2 L reactor, with particular attention paid to reaction time, temperature, and catalyst recyclability. Detailed characterization via ^{1}H NMR and FT-IR confirmed high conversion rates and product selectivity, although catalyst deactivation was observed, in particular in the synthesis of the glycerol carbonate pathway. Complementing the experimental work, a techno-economic analysis was performed, incorporating mass and energy balances, equipment sizing, and cost estimations. High return on investment (ROI) values were projected for all three products, under idealized assumptions. Overall, the study emphasizes the potential of CO_2-derived cyclic carbonates as sustainable alternatives to petrochemical counterparts while identifying key challenges such as high feedstock costs and catalyst longevity that must be addressed for industrial-scale applications.

2 Introduction

The transition toward sustainable resources is a key priority in modern chemical processes. Human activities such as electricity generation, transportation, and manufacturing have significantly increased emissions of greenhouse gases like carbon dioxide (CO_2), with serious repercussions for both the environment and human health [1]. The steady rise in atmospheric CO_2 levels has raised global concerns and spurred efforts to capture, store, or convert this gas into useful chemicals [2]. Although CO_2 is an appealing feedstock due to its low cost, non-toxicity, and renewability, it is also highly stable, as carbon is in its most oxidized state. This makes its transformation into valuable products a challenging endeavor [3].

One promising approach is utilizing CO_2 as a feedstock for producing valuable chemicals, thereby contributing to both carbon capture and the development of high-value products [4]. This study explores the cycloaddition of CO_2 to renewable epoxides to synthesize cyclic carbonates, which has garnered a lot of attention in the past years due to its atom-efficient reaction that can produce useful chemicals such as cyclic carbonates [5] [6]. Furthermore, cyclic carbonates are highly versatile; owing to their high boiling points, low toxicity, and polarity, they are employed as green solvents, monomers for polymer synthesis, and reactants for organic synthesis [7].

Three epoxides were selected for this study: allyl glycidyl ether (AGE), butylene oxide and glycidol. The selection criteria included their biobased nature, commercial availability, the maturity of biobased alternatives, and the feasibility of their conversion to cyclic carbonates. The research was conducted in two stages: first, reaction conditions were optimized in a 100 mL batch reactor to determine suitable parameters such as temperature and time for industrial application. Subsequently, the process was upscaled to a 2 L reactor to assess reproducibility and scalability.

Additionally, the recyclability of the Amberlite IRA-910 catalyst was evaluated, as it demonstrated the highest catalytic performance for these reactions. By systematically analyzing its performance over multiple reaction cycles, this study provides insights into the feasibility of CO_2-based cyclic carbonate production on an industrial scale.

3 Literature review

3.1 Selection of the Cyclic Carbonates

In this section, the selected cyclic carbonates are discussed with respect to three criteria: chemical and physical properties of the carbonate, availability of the epoxide, and bio-based nature. These criteria were chosen since they are fundamental to assess the upscaling feasibility of a bio-based process.

3.1.1 Allyl Glycidyl Carbonate

The Allyl Glycidyl Carbonate (AGC) is synthesized from the epoxide Allyl Glycidyl Ether (AGE) and carbon dioxide (Figure 1) [8].

Features and Properties of the Carbonate:
AGC, contains both an allylic double bond and an epoxide ring. The allylic double bond readily participates in electrophilic addition reactions while the epoxide ring is prone to nucleophilic ring-opening [9]. This dual reactivity allows AGC to serve as a versatile intermediate in various chemical processes. For example, when used as a co-monomer in the synthesis of styrene copolymers, AGC enhances the overall polymer properties such as flexibility, impact resistance, and adhesion [10]. One study demonstrated that incorporating AGC into a styrene copolymer resulted in materials that performed exceptionally well in coating and adhesive applications [10].

Feasibility of the Epoxide:
AGE, is a liquid at room temperature and is used in industrial applications, making it an attractive option for the synthesis of AGC. Currently, AGE is prepared commercially by the etherification of allyl alcohol with epichlorohydrin [11]. Hydrogen chloride, the by-product of their condensation is then removed by adding a base such as sodium hydroxide [12].

Bio-based Nature of the Epoxide:
AGE can be derived from biobased sources, improving the sustainability and environmental compatibility of its production. In a biobased process, the primary feedstocks are allyl alcohol and epichlorohydrin obtained from renewable resources rather than petroleum. For example, allyl alcohol can be produced via the catalytic dehydration of glycerol, which is a byproduct of biodiesel production [13]. Sustainable methods for producing epichlorohydrin from plant-based glycerol have also been developed. In these processes, glycerol is first converted to its dichlorohydrin derivatives by reaction with hydrochloric acid; these intermediates then undergo dehydrochlorination to yield epichlorohydrin. Importantly, the dehydrochlorination step is not simply the reverse of the hydrochlorination reaction but instead involves the elimination of hydrogen chloride to form the epoxide ring of epichlorohydrin, a structure that is distinct from the original glycerol molecule [14] [15]. Although these biobased production routes are currently at the laboratory or pilot scale, they hold considerable promise for enabling a greener synthesis of AGC.

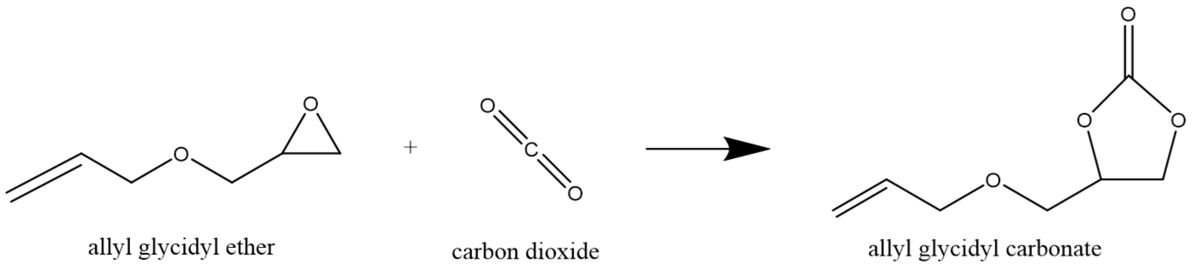

Figure 1: AGC Synthesis

3.1.2 Butylene Carbonate

Butylene carbonate is synthesized through the cycloaddition reaction of butylene oxide with carbon dioxide, forming a five-membered cyclic carbonate structure (Figure 2). The process offers a direct and efficient pathway to produce butylene carbonate [16].

Features and Properties of the Carbonate:
Butylene carbonate is a compound that remains fluid at room temperature and exhibits high chemical stability and excellent solvent properties. Its unique chemical structure not only facilitates effective mixing but also imparts enhanced thermal stability. These characteristics address it as a suitable candidate for applications as a solvent, adhesive component, and a renewable monomer in the synthesis of polymers such as polycarbonates and bio-polyurethanes [17] [18][19]. As the other cyclic carbonates discussed they seem like a promising alternative to petroleum-derived battery electrolytes, despite a moderate viscosity that may present challenges in some solvent applications [20][16].

Feasibility of the Epoxide:
Butylene oxide, the key epoxide precursor for butylene carbonate, demonstrates excellent reactivity with carbon dioxide, allowing high efficiency in cycloaddition reactions. The primary industrial production routes for butylene oxide are the chlorohydrin process, peroxyacetic acid process, and cumene hydroperoxidation process [21]. Alternatively, bio-based synthesis routes have been explored. These involve the fermentation of biomass to yield biobutanol, which is then dehydrated to produce butenes followed by an epoxidation step to generate butylene oxide[16]. Although the bio-based process aligns with green chemistry principles by utilizing renewable feedstocks, it remains in the early stages of development, with challenges in catalyst efficiency and process scale-up [22].

Bio-based Nature of the Epoxide:
The economic feasibility of bio-based butylene oxide is constrained by the high production costs of biobutanol and inefficiencies in the chemical conversion processes [22] [19]. In comparison, the petrochemical route remains the dominant method for butylene oxide production, driven by its well-established market, higher production efficiency, and significantly lower costs [23]. While bio-based butylene oxide offers a promising alternative for the future, its current economic and technical limitations prevent it from being viable at this stage. The challenges associated with biobutanol production and the conversion processes need to be addressed before large-scale implementation can be considered.

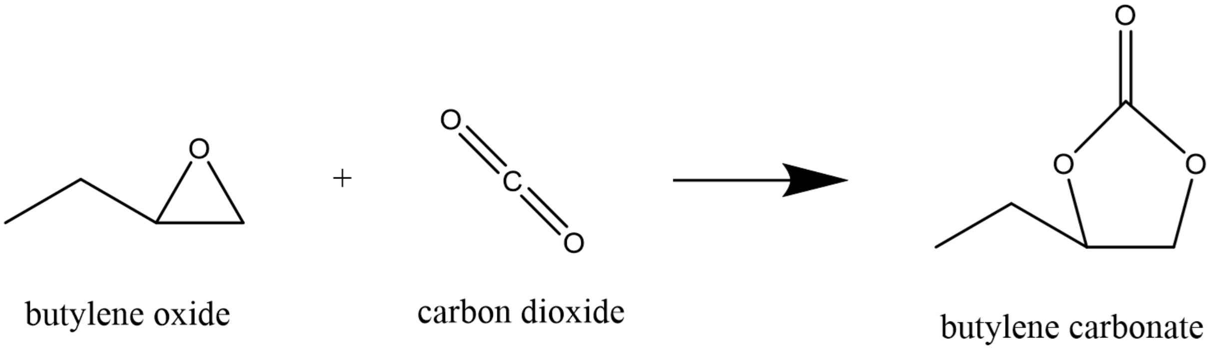

Figure 2: Butylene Carbonate Synthesis.

3.1.3 Glycerol Carbonate

Glycerol carbonate is synthesized from glycidol and carbon dioxide (Figure 3). The synthesis of glycerol carbonate has gained increasing attention due to its role as a sustainable alternative in various industrial applications [24].

Features and Properties of the Carbonate:
Glycerol carbonate is a bio-based compound that remains fluid at room temperature and exhibits favorable mixing properties. It is used as a solvent, lubricant, coating agent, and ingredient in pharmaceutical and personal care products [25][26]. Additionally, due to its chemical structure, glycerol carbonate serves as a crucial building block in organic and polymer chemistry [27]. Glycerol carbonate could be a useful substitute in batteries to petroleum-derived cyclic carbonate due to its environmentally friendly nature, high thermal stability, low toxicity, and strong electrochemical performance at both room and elevated temperatures [28]. Its biocompatibility and biodegradability make it an attractive alternative to petroleum-derived carbonates [29].

Feasibility of the Epoxide:
Glycidol can be synthesized through both petrochemical and bio-based pathways. The conventional petrochemical route involves the epoxidation of allyl alcohol using hydrogen peroxide, achieving high selectivity but relying on fossil-based feedstocks propylene and propylene oxide [30]. Alternatively, bio-based glycidol can be derived from glycerol, a by-product of biodiesel production. One common approach involves the chlorination of glycerol to produce epichlorohydrin, which is then dehydrochlorinated to yield glycidol [31]. As explained earlier bio-based epichlorohydrin can be made from the glycerol through a two-step process, involving its hydrochlorination followed by dehydrochlorination in the gas phase [15].

Bio-based Nature of the Epoxide:
Although current bio-based production methods for glycidol are primarily in laboratory or pilot-scale settings, considerable potential exists for industrial scale-up [32]. The conventional petrochemical route, typically involving the oxidation of propylene oxide, has been long established and remains more cost-effective at present [24]. However, the direct conversion of glycerol to glycidol via glycerol carbonate decarboxylation presents a promising bio-based alternative, with high atom efficiency and reduced environmental impact. Further advances in catalyst design and process optimization are essential for making this method competitive with fossil-based routes. Moreover, supportive regulatory measures, such as subsidies and carbon credit schemes, could play a pivotal role in transitioning these emerging technologies to full industrial application [29].

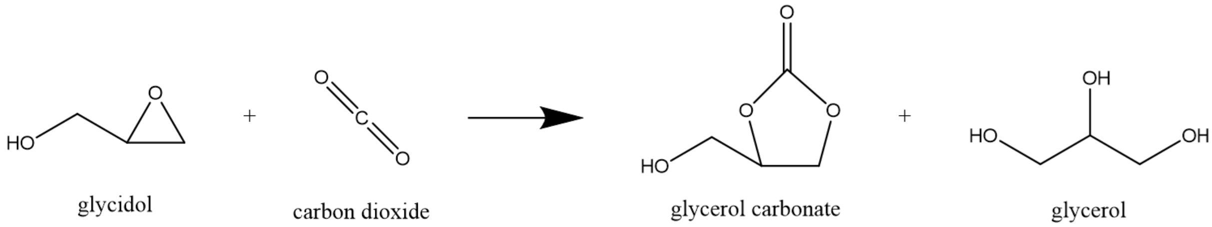

Figure 3: Glycerol Carbonate Synthesis.

3.2 Catalyst selection

The selection of an appropriate catalyst is crucial for the efficient conversion of epoxides to cyclic carbonates. In this study, Amberlite resins were chosen for the synthesis of cyclic carbonates based on several key factors, including their metal-free composition, ease of separation, and high efficiency in epoxide conversion. These characteristics align with the principles of green chemistry, promoting sustainability and minimizing environmental impact.

Amberlite catalysts consist of polystyrene resins that are cross-linked with divinylbenzene. These resins can be modified with different functional groups, such as imidazolium-based ionic liquids and phosphonium halides. These functional groups serve as active catalytic sites and nucleophiles in the reaction [33]. Based on the research by Yasser et al., two Amberlite-based catalysts, Amberlite IRA-900 and Amberlite IRA-910, have demonstrated efficient performance in the production of cyclic carbonates [34]. In this research, the most suitable Amberlite catalyst will be selected for further testing. Once identified, its catalytic pathway will be analyzed and explained in detail.

Among the evaluated catalysts, Amberlite IRA-910 ion-exchanged with iodide has been identified as the most effective for the synthesis of carbonates from epoxides. This selection is based on its superior catalytic performance in terms of yield and selectivity compared to alternative catalysts. According to Yasser et al., this catalyst demonstrated the highest efficiency in the catalytic conversion of styrene oxide to styrene carbonate, achieving a yield of 59% with a selectivity of 99% while the other catalyst the Amberlite IRA-900 remaining at 12% conversion [34].

Furthermore, Yasser et al [34], investigated the role of water as a hydrogen bond donor (HBD) in enhancing catalytic activity. Their findings indicated that the optimal amount of water to be added to the reaction was 0.02 mL. The addition of water led to an increase in yield from 59% to 64%, although a slight decrease in selectivity was observed, from 99% to 98% [34].

Based on these findings, Amberlite IRA-910 ion-exchanged with iodide will be employed in subsequent catalytic tests to further assess its performance and potential for scale-up applications.

Additionally the study by Yasser et al., reported that the catalytic activity of their Amberlite-based system decreased over successive reaction cycles. In their experiments, the yield of styrene carbonate dropped from 65% in the first run to 55% in the fourth run. The catalyst was easily recovered through simple filtration, as the resin beads' size allowed for straightforward separation from the reaction mixture[34].

In light of these findings, the potential deactivation of the catalyst due to ion exchange phenomena raises concerns about its long-term performance. In this study, recycling tests will be performed using three selected substrates: AGC, butylene carbonate, and glycerol carbonate, under our optimized conditions. These tests aim to further assess the catalyst's stability and reusability, offering deeper insight into the underlying deactivation mechanisms.

3.2.1 Catalytic Pathway

A proposed catalytic pathway outlines how the Amberlite catalyst facilitates the conversion of epoxides into cyclic carbonates,(Figure 4, adapted from [34]). The mechanism emphasizes the synergistic roles of the catalyst's hydroxyl groups, iodide ions, and water in driving the reaction.

Catalyst Structure and Functionality
The Amberlite IRA-910 catalyst features a hydroxyl (-OH) group anchored to its polymeric support (Figure 4). This structure enhances catalytic activity during cyclic carbonate synthesis, likely by stabilizing intermediates through hydrogen. The Amberlite IRA-910-catalyzed formation of cyclic carbonate from epoxide and CO_2 proceeds via four key steps (Figure 5, adapted from [34]):

1 Epoxide Activation:
The catalyst's hydroxyl group interacts with a water molecule, forming a hydrogen-bonded network. In parallel with water coordinating the OH, the epoxide interacts with the active sites of the Amberlite IRA-910 by coordination of the oxygen-densely charged (-) of the epoxide with the ammonium group. This induces ring opening, generating an alkoxide intermediate.

2 CO_2 Insertion:

The alkoxide intermediate formed undergoes nucleophilic attacks on the electrophilic carbon of CO_2, forming a carbonate species. This step is rate-limiting due to the kinetic inertness of CO_2.

3 Cyclization:
The carbonate intermediate undergoes cyclization. Here, the oxygen atom replaces the iodide ion, forming a cyclic carbonate ring and releasing I-.

4 Catalyst Regeneration:
The liberated iodide ion recombines with the catalyst, restoring its active form for subsequent catalytic cycles.

Key Insights: This pathway shows the dual role of the catalyst: (1) iodide serves as a nucleophile to initiate epoxide ring opening, and (2) the Hydroxylated support stabilizes transition states via hydrogen bonding. Water mediates proton transfer steps, while CO_2 is efficiently incorporated into the final product.

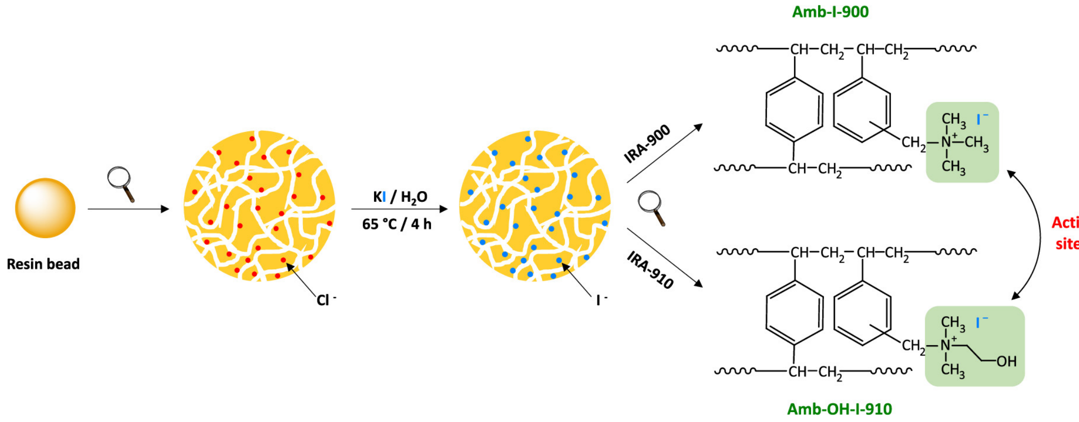

Figure 4: Synthesis of the Amberlite IRA-900 and Amberlite IRA-910 Catalysts in Bead Format by Ion Exchange. Taken from Yasser et al [34].

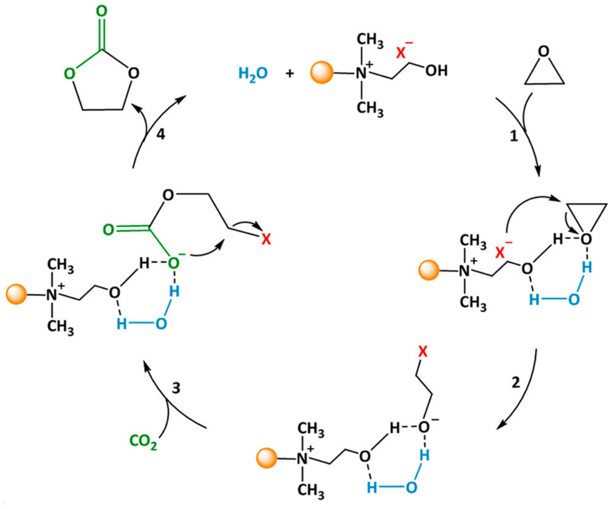

Figure 5: Proposed Mechanism for the Cycloaddition Reaction of CO_2 to an Epoxide over Amberlite IRA-910 in the Presence of Water as HBD. Taken from Yasser et al [34].

3.3 Techno-economic analysis

The techno-economic analysis of cyclic carbonate synthesis evaluates the feasibility of industrial-scale production by analyzing costs, material availability, process efficiency, and market viability. This section reviews relevant literature on the cost-effectiveness of cyclic carbonate synthesis, the economic potential of bio-based feedstocks, and advancements in catalyst development that influence scalability.

3.3.1 Economic considerations

The economic feasibility of cyclic carbonate production depends on several factors: feedstock availability and cost, reaction efficiency, catalyst lifespan, energy requirements, and market demand. Literature suggests that the cycloaddition of CO_2 to epoxides is a promising route for sustainable chemical production [35].

3.3.2 Price of the materials

A key determinant of economic viability is the cost of epoxides and CO_2. While fossil-derived epoxides continue to dominate the market, bio-based alternatives are emerging. As discussed in the previous sections, the reactants for epoxide production can be derived from renewable sources. However, the high cost of bio-based epoxides compared to petrochemical routes currently limits large-scale adoption [31]. Advances in bio-based feedstocks are necessary to reduce production costs and make bio-derived feedstocks more competitive.

For this reason, the prices of epoxides derived from fossil sources will be listed (Table 1). For CO_2, a price of 0.20 €/kg is assumed, based on the premise that utilizing CO_2 from industrial sources contributes to emission reduction efforts. The associated cost is relatively small and accounts for purification and pressurization, assuming the CO_2 is supplied at a pressure of 10 bar with 99.8% purity. The cost of electricity is assumed to be 0.07 €/kWh, based on wholesale energy pricing [36].

Table 1: Costs of materials per kilogram.

Material	Price (€/kg)	Reference
Glycidol	278	[37]
Glycerol carbonate	1022	[38]
Allyl glycidyl ether	236	[39]
Allyl glycidyl carbonate	147.000	[40]
Butylene oxide	71	[41]
Butylene carbonate	1160	[42]
Water (deionized)	0,82	[43]
Acetone	0,817	[44]
Amberlite IRA-910 (chloride form)	16	[45]
Carbon dioxide	0,2	-
Potassium iodide	172,5	[46]

3.3.3 Catalyst choice

The choice of catalyst significantly influences process economics. Metal-based catalysts, while efficient, contribute to high operational costs due to their expense and potential deactivation over time. Recent studies have explored the use of metal-free heterogeneous catalysts such as Amberlite IRA-910, which offer advantages in recyclability and cost reduction [34]. The economic analysis of catalyst reuse cycles is critical, as the ability to maintain high conversion rates over multiple cycles directly impacts process sustainability.

3.4 Market potential

The market for cyclic carbonates is expanding as industries seek greener alternatives to conventional petrochemical products. According to Pescarmona [47], cyclic carbonates are gaining traction due to their potential to replace toxic reactants and their increasing use in energy storage applications.

Despite their advantages, the widespread adoption of cyclic carbonates faces economic hurdles. While large-scale production remains reliant on petrochemical feedstocks, research efforts are directed toward developing cost-competitive bio-based pathways. The synthesis of ethylene and propylene carbonates from biomass-derived ethanol and propylene is under exploration, with potential for industrial implementation once economic viability improves [47].

Additionally, regulatory policies and carbon pricing mechanisms could enhance the economic feasibility of CO_2-derived cyclic carbonates. The introduction of carbon credits and subsidies for carbon capture and utilization (CCU) technologies may provide financial incentives for manufacturers to adopt greener synthesis routes [48].

4 Experimental section

4.1 Materials

Glycidol (96%), potassium iodide (≥99%), Amberlite IRA-910 chloride form, mesitylene (98%), trimethoxybenzene (≥99%), trioxane (≥99%), deuterated chloroform ($CDCl_3$, 99.6 atom%), and deuterated dimethyl sulfoxide-d$_6$ (DMSO-d$_6$, 99.5% atom), used as solvents for ^{1}H NMR analysis, were purchased from Sigma-Aldrich. Allyl glycidyl ether (AGE, ≥ 99%) and 1,2-butylene oxide (≥ 99%) were obtained from TCI Chemicals.

4.2 Catalytic Test

4.2.1 Catalyst Preparation

Ion exchange was carried out using a heated glycerol bath and a 500 mL round-bottom flask. The preparation of Amberlite IRA-910 required a double ion exchange process. A solution of KI (50 g, 300 mmol) in water (100 mL) was placed in a 500 mL one-neck round-bottom flask equipped with a magnetic stirrer. Then, 10 g of Amberlite IRA-910 resin beads in chloride form were added to the solution. This mixture was stirred at 65°C for 4 hours.

After completion, the solution was transferred to an ice bath and allowed to cool to room temperature. The Amberlite IRA-910 catalyst was recovered using a sintered glass Büchner funnel, then washed with 4 × 100 mL of water followed by 2 × 60 mL of acetone. The resulting resin beads were dried overnight in an oven at 70°C for at least 14 hours. After this initial drying step, the ion exchange process was repeated to ensure complete exchange. The resulting Amberlite IRA-910 beads underwent a second drying step in the oven at 70°C for 48 hours.

4.2.2 100 mL Batch Reactor

The tests were conducted in a high-pressure, high-temperature 100 mL Parr reactor (Figure 8) at the University of Groningen. This reactor can operate at temperatures up to 200°C and pressures up to 250 bar. The temperature is regulated via a heated water system with precise control.

4.2.3 2 L Batch Reactor

The tests were also conducted in a high-pressure, high-temperature 2 L Parr reactor (Figure 7) at the University of Groningen. This reactor can operate at temperatures up to 200°C and pressures up to 100 bar. The system is equipped with a stirrer, and the temperature is regulated via an internal control system using electrical heating cartridges.

4.2.4 Preliminary Catalyst Procedure

In the 100 mL reactor experiments, the procedure was as follows: the required amounts of epoxide, water, and the Amberlite IRA-910 catalyst were introduced into the reactor, which was then sealed with clamps. The reactor was pressurized at room temperature, stirred, and heated to the target temperature. Once this temperature was reached, the reaction began. After completion, the reactor was allowed to cool to room temperature, depressurized to 0 bar, and the reaction mixture was collected in a vial for NMR analysis (see Section 4.2.6).

4.2.5 Scale-Up to a 2 L Reactor and Subsequent Recycling Tests

For the scale-up experiments, the required amounts of epoxide, water, and Amberlite IRA-910 catalyst were first added to the 2 L reactor. The reactor was then sealed with the appropriate clamps, pressurized to the desired level, and stirred. After pressurizing the reaction, heating was initiated until the set temperature was reached. After the designated reaction time, the reactor was cooled to room temperature by removing the heating element and then depressurized to 0 bar. The reaction mixture was transferred to a vial, and an NMR sample was prepared (section 4.2.6).

Recycling tests were performed using the 2 L reactor to simulate a factory setting, where the reaction mixture is removed while the catalyst remains in the reactor for subsequent batches. In this process, the reaction liquid is drained from the reactor, leaving the catalyst behind. The catalyst is then filtered through a sintered glass Büchner funnel to separate it from any residual reaction mixture. Finally, the catalyst is returned to the reactor, and a new batch is initiated by adding the epoxide (and water if required) for the reaction.

4.2.6 H-NMR Analysis

The Varian Oxford 300 MHz or the Varian Mercury 400 MHz NMR spectrometer was used to conduct the H-NMR analysis. H-NMR samples were prepared by dissolving approximately 50 mg of the reaction mixture in 600 mg of solvent. For the glycerol carbonate synthesis, DMSO-d_6 was used as the solvent, and for the butylene and allyl glycidyl carbonate syntheses, chloroform was utilized. The reaction mixture's yield, conversion, and selectivity were determined using the following formulas:

Epoxide Conversion %:

$$\text{Epoxide Conversion\%} = 100\times\left(1 - \frac{\text{mol of remained epoxide}}{\text{mol of cyclic carbonate} + \text{mol of remained epoxide} + \text{mol of diol, if present}}\right) \tag{1}$$

Cyclic Carbonate Yield %:

$$\text{Cyclic Carbonate Yield\%} = 100\times\left(\frac{\text{mol of product}}{\text{mol of cyclic carbonate} + \text{mol of remained epoxide} + \text{mol of diol, if present}}\right) \tag{2}$$

Cyclic Carbonate Selectivity %:

$$\text{Cyclic Carbonate Selectivity\%} = \left(\frac{\text{Carbonate Yield}}{\text{Epoxide Conversion}}\right) \times 100 \tag{3}$$

The molar quantities of epoxide, cyclic carbonate, and diol (if present) were determined by integrating the respective peaks of each compound rather than relying on the internal standard peaks. Since deviations in the mass balance of the internal standards exceeded 10%, it was decided to use the ratios between the formed carbonate, epoxide, and diol (if present) as the basis for quantification. An example calculation is provided in Appendix 3.

A limitation of this approach is that the mass balance will always sum to 100%. however, it is considered more reliable than using internal standards. Several internal standards were tested in this study, including mesitylene, 1,3,5-trimethoxybenzene, and 1,3,5-trioxane. However, all of them exhibited deviations in their mass balance greater than 10%. As a result, the ratios between the epoxide and carbonate were selected as the most reliable method for quantification.

4.2.7 FT-IR

Fourier transform infrared (FT-IR) spectra were recorded on an IRTracer-100 spectrometer by averaging 64 scans with a Wavenumber 4000 to 600 cm^{-1} for the characterization of the catalyst, an elemental analysis was performed.

FT-IR spectroscopy was used to identify the chemical functional groups present in the catalyst [49]. This characterization provides insight into the compounds remaining on the catalyst surface, offering valuable information about their composition and any possible side products formed.

5 Results

In this section, the results obtained during my thesis will be presented and discussed. The findings are organized into several key areas, beginning with the catalyst synthesis, followed by a detailed analysis of the three different substrates: AGC, butylene carbonate, and glycerol carbonate. Each substrate will be explored in three distinct parts: first, the process validation, where the results will be compared to existing literature; second, the optimization, which will cover the adjustments made to improve the cyclic carbonate production; and third, the recycling tests, focusing on the reuse and sustainability of the catalyst. Additionally, a techno-economic analysis will be presented to assess the economic feasibility and potential for scaling up to an industrial level.

5.1 Catalyst synthesis

The Amberlite IRA-910 beads in iodide form were prepared through a two-step ion exchange process of Amberlite IRA-910 resin in the chloride form. The resin consists of polystyrene cross-linked with divinylbenzene and functionalized with dimethyl ethanol ammonium chloride groups (Figure 4). The resin is commercially available and consists of small beads with a size distribution of 530–800 µm. No degradation of the catalyst was observed during the ion exchange process. The catalyst synthesis was successful, resulting in usable Amberlite IRA-910 resin for cyclic carbonate synthesis. Elemental analysis of the catalyst was also conducted using FT-IR and is further discussed in subsection 5.5.

5.2 Validation of AGC Synthesis

The primary objective of this validation was to replicate the results reported by Yasser et al. [34]. Their procedure was followed precisely—with the sole modification that, while Yasser et al. prepared the Amberlite IRA-910 catalyst using a single ion exchange step, the current study employed a two-step ion exchange process. In every experiment, the reaction was conducted at 80 °C for 18 hours, with a molar ratio of 1.82 epoxide to CO_2. The catalyst was loaded at 3% by weight relative to the epoxide, and water, acting as a hydrogen bond donor (HBD), was added at a 3% mass ratio relative to the epoxide. Replicating these conditions was expected to yield comparable results.

In addition, the synthesis of AGC was carried out according to the procedure described in [34]. In the original work, a yield of 65% was reported, with a selectivity $\geq$ 99% and no detectable side products in the ^{1}H NMR spectra; notably, these experiments were performed in a 10-block reactor. Here, we present our experimental data for AGC synthesis, which confirms the reproducibility of the reported results under our laboratory conditions.

This was the first reaction to be replicated. This experiment was conducted in the 100 mL batch reactor (slightly larger than the 84 mL reactor used by Yasser et al.). By maintaining the same molar ratios as reported, a conversion and yield of 75% were achieved under identical reaction conditions (Table 3, entry 1). The conversion, yield, and selectivity were determined as described in Section 4.2.6. The ^{1}H NMR spectra of the cyclic carbonates are provided in Appendix 2.

5.2.1 Optimization of AGE

This section examines how reaction conditions can be adjusted to facilitate scaling up to industrial levels. The first optimization step involved increasing the temperature to 100°C, a modification that, as previously reported in by Yasser et al., for the synthesis of styrene carbonate, positively influenced yield [34]. In this paper, the yield of styrene oxide increased from 66% to 93%, which is a significant improvement and would be beneficial for our synthesis. After increasing the temperature, the reaction time was systematically reduced to enhance process efficiency while targeting 100% conversion and yield. The temperature increase was initially performed in a 2L reactor, with subsequent optimization tests conducted in the 100 mL batch reactor. Final validation was then carried out in the 2L reactor (Table

4, entries 1 and 2). For AGC synthesis, raising the temperature to 100°C markedly improved both yield and conversion to ≥99% compared to the initial 75% conversion and yield at 80°C.

The next step was to reduce the reaction time (Table 3, entries 2 and 3). A reduction of the reaction time to 5 hours resulted in a 94% conversion and yield, and extending the time to 7 hours achieved ≥99% conversion and yield. This was a very good result, with both conversion and yield improved while reducing reaction time. As a result, the process was now ready to be performed in the 2L reactor for the final recycling steps.

5.2.2 2L validation and Recycling test

Three recycling runs for AGC synthesis were conducted using the optimized conditions (Table 4, entries 3-5). During the first run (Table 4, entry 3) the reaction was a success, achieving the same yield and conversion of 98%. The recycling runs were then started as described in 4.2.5. During the second run (Table 4, entry 4) a conversion and yield of 97% were achieved. However, a decrease in catalytic activity was observed in the third run (Table 4, entry 5), with conversion dropping to 94%. These results suggest that the catalyst remains effective for up to two cycles before experiencing deactivation.

Table 2: The effect of cycle loading CO_2 to AGE using the Amberlite IRA-910 catalyst with water in a 100 mL batch reactor.

Entry	Time (h)	Temperature (°C)	Conversion (%)	Yield (%)	Selectivity (%)
1	18	80	65	65	≥ 99
Reaction conditions: Epoxide (20 mmol), Amberlite IRA-910 catalyst (95 mg, 0.21 mmol I), water (0.02 mL), mesitylene (1.5 mmol) as ^{1}H NMR internal standard, 10 bar CO_2, 80 °C, 18 h.					

Table 3: The effect of cycloaddition of CO_2 to AGE using the Amberlite IRA-910 catalyst with water in a 100 mL batch reactor.

Entry	Time (h)	Temperature (°C)	Conversion (%)	Yield (%)	Selectivity (%)
1	18	80	75	75	≥ 99
2	5	100	94	94	≥ 99
3	7	100	≥ 99	≥ 99	≥ 99
Reaction conditions: AGE (78 mmol), Amberlite IRA-910 catalyst, and water (3 wt% relative to AGE). CO_2 pressure: 46 bar.					

Table 4: The effect of the cycloaddition of CO_2 to AGE using the Amberlite IRA-910 catalyst with water in a 2 L batch reactor.

Entry	Time (h)	Temperature (°C)	Conversion (%)	Yield (%)	Selectivity (%)
1	18	80	68	68	≥ 99
2	18	100	≥ 99	≥ 99	≥ 99
3	7	100	98	98	≥ 99
4	7	100	97	97	≥ 99
5	7	100	94	94	≥ 99
Reaction conditions: AGE (1.2 mol), Amberlite IRA-910 (3 wt% relative to the epoxide weight), water as HBD (3 wt% relative to the epoxide), 35 bars CO_2.					

5.3 Butylene carbonate

The next substrate to be explored is butylene oxide, which will follow the same procedure as the previously studied substrate, AGE. The process will first be validated under the reaction conditions, followed by optimization of the synthesis. This will lead to a final validation using the 2L reactor, along with recycling tests to assess process efficiency and sustainability.

5.3.1 Validation of butylene carbonate synthesis

The First synthesis of butylene carbonate used the same reaction conditions as the AGE synthesis. For the conversion of butylene oxide, a yield, and conversion of 57% was obtained (Table 5, entry 1). The utilization of this method shows worse results compared to the AGC synthesis. These outcomes provide a solid basis for further optimization.

5.3.2 Optimization of Butylene Carbonate Synthesis

For butylene carbonate, increasing the reaction temperature to 100°C resulted in ≥99% conversion and yield (Table 6, entries 1 and 2). A reduction of the reaction time from 18 hours to 6 hours initially produced a conversion of 97% (Table 5, entry 2), thereby initially establishing 6 hours as the optimal reaction time for this substrate in the 100 mL batch reactor.

5.3.3 Recycling Tests for Butylene Carbonate

For butylene carbonate, the first recycling synthesis in the 2L reactor (Table 6, entry 3) resulted in a yield reduction of 88%. However, three successive recycling runs were conducted under the optimized conditions, with the yield remaining around 90%. A slight decrease in efficiency was observed when scaling up from the 100 mL batch reactor to the 2L reactor, as the 100 mL reactor had previously achieved 97% conversion and yield in a 6-hour run (Table 5, entry 2). To address this, an additional run was performed (Table 6, entry 6) with an extended reaction time of one hour, leading to an increase in yield and conversion to 98%. This differs from the results obtained in AGC synthesis, as no catalyst deactivation was observed during recycling, indicating that the process has potential for industrial-scale application.

Table 5: The effect of the cycloaddition of CO_2 to butylene oxide using the Amberlite IRA-910 catalyst with water in a 100 mL batch reactor.

Entry	Time (h)	Temperature (°C)	Conversion (%)	Yield (%)	Selectivity (%)
1	18	80	57	57	≥ 99
2	6	100	97	97	≥ 99
Reaction conditions: Butylene oxide (100 mmol), Amberlite IRA-910 (3 wt% relative to the epoxide weight), water as HBD (3 wt% relative to the epoxide), pressure of 59 bar CO_2.					

Table 6: The effect of the cycloaddition of CO_2 to butylene oxide using the Amberlite IRA-910 catalyst with water in a 2 L batch reactor.

Entry	Time (h)	Temperature (°C)	Conversion (%)	Yield (%)	Selectivity (%)
1	18	80	57	57	$\geq$ 99
2	18	100	$\geq$ 99	$\geq$ 99	$\geq$ 99
3	6	100	88	88	$\geq$ 99
4	6	100	90	90	$\geq$ 99
5	6	100	92	92	$\geq$ 99
6	7	100	98	98	$\geq$ 99
Reaction conditions: Butylene oxide (1.6 mol), Amberlite IRA-910 (3 wt% relative to the epoxide weight), water as HBD (3 wt% relative to the epoxide), 47 bars CO_2.					

5.4 Glycerol carbonate

The last substrate to be synthesized is glycerol carbonate. This process will follow the same steps as the previously explored substrate, AGC and butylene carbonate. First, the process will be validated using the reaction conditions. Then, subsequent optimization of the synthesis will be carried out, followed by final validation in the 2L reactor and recycling tests.

5.4.1 Glycerol carbonate validation

After replicating the AGC results, identical reaction conditions were applied to the synthesis of glycerol carbonate glycerol carbonate synthesis achieved high conversion (≥99%) and yield (96%) of glycerol carbonate, the selectivity was limited due to the formation of glycerol as a side product (Table 7, entry 1). These outcomes provide a solid basis for further optimization.

5.4.2 Optimization of Glycerol Carbonate Synthesis

Although glycerol carbonate synthesis achieved full conversion at the initial conditions, the temperature was increased to 100°C to evaluate its effect on selectivity. Due to the inherent water content of glycidol, a side reaction leading to glycerol formation occurs. An increase in yield from 82% to 88% was observed (Table 8, entries 1 and 2). These optimization tests achieved a lower yield compared to the result achieved in the 100 mL batch reactor (Table 7, entry 1), where a yield of 96% was achieved. At 100°C, a 6-hour reaction maintained full conversion with a yield of 84% (Table 7, entry 2). A further reduction to 1.5 hours yielded similar results, and a final reduction (Table 7, entry 4) to 45 minutes resulted in a yield of 87% with a conversion of ≥99%. The 45-minute reaction was selected as the final test condition.

5.4.3 Recycling Tests for Glycerol Carbonate

Four recycling tests for glycerol carbonate were performed (Table 8, entries 3-6) under the validation conditions (Table 7, entry 4), with a slight modification: no water was added to the epoxide as HBD, since glycidol already contains hydroxyl groups that can facilitate the hydrogen bonds. The results showed that the first two cycles maintained ≥99% conversion with a selectivity of 91% toward the desired glycerol carbonate (Table 8, entries 3 and 4). A decline was observed in the third cycle (Table 8, entry 5), where conversion fell below 91% and the yield decreased to 88%, followed by a further decline to 70% conversion and 67% yield in the fourth run (Table 8, entry 6). These results suggest that the catalyst remains effective for up to two cycles before experiencing deactivation.

Table 7: The effect of the cycloaddition of CO_2 to glycidol using the Amberlite IRA-910 catalyst with water in a 100 mL batch reactor.

Entry	Time (h)	Temperature (°C)	Conversion (%)	Yield (%)	Selectivity (%)
1	18	80	≥ 99	96	96
2	6	100	≥ 99	84	84
3	1.5	100	≥ 99	84	84
4	0.75	100	≥ 99	87	87
Reaction conditions: glycidol (110 mmol), Amberlite IRA-910 (3 wt% relative to epoxide weight), water (3 wt% relative to epoxide), 65 bar CO_2.					

Table 8: The effect of the cycloaddition of CO_2 to glycidol using the Amberlite IRA-910 catalyst with water in a 2 L batch reactor.

Entry	Time (h)	Temperature (°C)	Conversion (%)	Yield (%)	Selectivity (%)
1	18	80	≥ 99	82	82
2	18	100	≥ 99	88	88
3	0.75	100	≥ 99	91	91
4	0.75	100	≥ 99	91	91
5	0.75	100	91	88	97
6	0.75	100	70	67	95
Reaction conditions: glycidol (2.2 mol), Amberlite IRA-910 (3 wt% relative to epoxide weight), water (3 wt% relative to epoxide)(entries 1 and 2), 64 bar CO_2.					

5.5 FT-IR Analysis of the Catalyst

FT-IR analyses were performed both before and after the recycling tests to examine the functional groups remaining on the catalyst. For each spent catalyst, two FT-IR spectra were recorded: one from the catalyst that was dried but not washed, and another from the catalyst that was both washed and dried. The drying process lasted for 14 hours. The catalyst was washed four times with 40 mL of water, followed by two washes with 30 mL of acetone to remove other functional groups and identify any residual functional groups that might indicate catalyst deactivation.

Notably, the catalyst exhibited distinct color changes depending on the substrate. In AGC synthesis, the catalyst turned very dark, almost black, while in glycerol carbonate synthesis, it developed a brownish tint that closely resembled the reaction mixture. In butylene carbonate synthesis, only slight yellowing was observed. After washing the catalyst, the colors also changed: for AGC synthesis, it became more grey, while for glycerol carbonate, it turned almost white with a slight yellow tint. In butylene carbonate synthesis, the catalyst returned to its original color. These color variations prompted the FT-IR study, which aimed to correlate these changes with possible alterations in the catalyst's structure. Detailed FT-IR spectra can be found in Appendix 4. These color changes of the catalyst can be observed in Appendix 5.

The FT-IR spectra revealed two major peaks: one around 1100 cm^{-1} and another near 1700 cm^{-1}. The peak at 1100 cm^{-1} is assigned to the stretching vibration of carbon-oxygen (C–O) bonds. This vibration is characteristic of ether or carbonate functionalities, which may arise from the epoxide ring opening or the formation of carbonate linkages [50]. The peak at approximately 1700^{-1} corresponds to the stretching vibration of carbonyl (C=O) bonds. This band is typical for ester or carbonate groups, where the C=O bond undergoes a stretching motion, confirming the presence of such functionalities on the catalyst surface [50].

5.5.1 AGC catalyst

During the recycling test, a small deactivation of the catalyst was observed. This deactivation was further examined using FT-IR analysis to look for changes in the surface functional groups. The FT-IR spectrum of the used AGC synthesis catalyst displays two prominent absorption bands: one centered near 1700 cm^{-1} and the other around 1100 cm^{-1} (Figure 15). The band at 1700 cm^{-1} is attributed to the stretching vibration of the carbonyl (C=O) group. This strong, sharp absorption is typical for ester or carbonate functionalities, where the double bond between carbon and oxygen undergoes a stretching motion due to the polarity introduced by the oxygen atom. This is related to the AGC. Meanwhile, the band at 1100 cm^{-1} corresponds to the stretching vibration of the carbon-oxygen (C-O) bond, a motion commonly associated with ether-like or carbonate groups such as those present in AGE or AGC.

After the washing procedure, the intensities of these peaks nearly return to that characteristic of the pure catalyst. However, a slight residual absorption remains at 1100 cm^{-1}, suggesting that a small amount of carbonate groups is still retained on the catalyst surface (Figure 16). This residual presence correlates well with the observed color change of the catalyst from black to grey, indicating that some material, likely containing the carbonate functionality, remains adsorbed even after washing.

5.5.2 Butylene carbonate

For the butylene carbonate synthesis, the FT-IR analysis indicates that the catalyst suffers no significant deactivation. The only observed change is a deepening of the absorption band around 1100 cm^{-1} (Figure 17). This band, corresponding to the stretching vibration of the carbon-oxygen (C-O) bond, shows the presence of carbonate or ether functionalities. The minor increase in the band's intensity suggests that not all of the carbonate species were completely removed during the washing step. Nonetheless, when compared with the spectrum of the pure catalyst, this slight modification aligns with expectations from the recycling tests and confirms that the catalyst retains its structural integrity and activity.

5.5.3 Glycerol carbonate

In contrast, the FT-IR analysis of the glycerol carbonate catalyst shows clear signs of deactivation. The spectrum of the unwashed glycerol carbonate catalyst displays more noticeable changes in the two main absorption bands at 1700,cm^{-1} and 1100,cm^{-1}. The stronger band at 1700,cm^{-1}, caused by the stretching vibration of the carbonyl (C=O) group, suggests that extra polycarbonate species have formed on the catalyst surface (Figure 19). This change is more pronounced than compared to butylene carbonate and AGC, indicating a greater level of deactivation likely due to the accumulation of polycarbonate materials that block the active sites.

Similarly, the intensified band at 1100,cm^{-1}, which is related to the stretching vibration of the C–O bond, points to the presence of carbonate groups and possible side products from glycerol reactions. After washing the catalyst, the 1700,cm^{-1} band decreases in intensity, implying that some of the polycarbonate deposits have been removed (Figure 20). However, the continued presence of signals in both bands indicates that possibly glycidol, glycerol carbonate, or glycerol derived polycarbonate remains strongly attached to the catalyst surface. This residue may be responsible for the color change observed in the reaction mixture and likely plays a key role in the overall deactivation during the recycling process.

5.6 Color change of the reaction mixture of glycerol carbonate synthesis

During the conversion of glycidol to glycerol carbonate using Amberlite IRA-910 as the catalyst, a marked coloration is observed both in the reaction mixture and on the catalyst surface (Figure 6). Although pure glycerol carbonate and glycerol are expected to be colorless, the reaction initially produces a very dark orange hue. With successive reuses of the Amberlite IRA-910 catalyst, this intense color gradually lightens to yellow. Such a color change is indicative of a decreasing concentration of the species responsible for the color change, which may stem from a polymerization side reaction involving glycidol, glycerol carbonate, or glycerol. It is plausible that glycerol polycarbonate (or related oligomers) forms during the reaction, as suggested by the observed darkening.

The initial hypothesis was that the color change resulted from the formation of a polycarbonate. ^{1}H NMR analysis was performed to search for peaks of the possible formed polycarbonate; however, aside from a noticeable water peak in DMSO between 3.3 and 3.4 ppm, no significant differences were detected (Figure 12). Thus, the proton ^{1}H NMR results alone do not conclusively explain the phenomenon, possibly due to peak overlap with the reaction products.

Furthermore, FT-IR analysis confirms that by-products still remain on the Amberlite IRA-910 catalyst even after the washing process. A clear absorption band at around 1100,cm^{-1} is observed, which corresponds to the stretching vibration of carbon–oxygen (C–O) bonds found in polycarbonate structures. At the same time, the lower intensity of the carbonyl (C=O) stretching band at around 1700,cm^{-1} suggests a decrease in the glycerol carbonate content on the catalyst surface. This combination of spectral features supports the idea that new functional groups are forming through side reactions. To fully understand the chemical nature and origin of these polymeric by-products, further analysis using complementary techniques such as mass spectrometry (MS), or X-ray Photoelectron Spectroscopy (XPS) is needed.

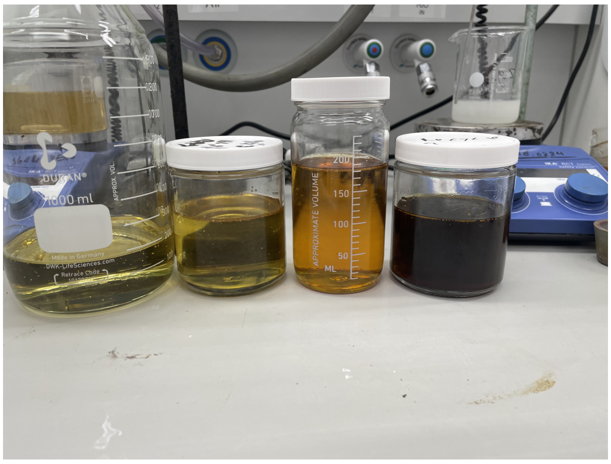

Figure 6: Reaction mixture glycerol carbonate synthesis color change Across Multiple Synthesis: Progressing from Fresh to Used Catalyst (right to left).

5.7 Techno-economic analysis

This study assesses the industrial feasibility of producing cyclic carbonates on a large scale, targeting an annual production volume of approximately 10.000 tonnes for each fine chemical product. The process is divided into two primary sections: (1) the synthesis of an ion-exchange catalyst (Amberlite IRA-910) via a dedicated ion-exchange procedure, and (2) the subsequent carbonation reaction that converts epoxides into cyclic carbonates.

A techno-economic analysis was conducted to evaluate the scalability of synthesizing three cyclic carbonates: AGC, butylene carbonate, and glycerol carbonate. Mass balance calculations were performed using an Excel-based model that incorporates established formulas from the literature [51] (Sinnott and Towler). Reactor designs and specifications were derived from the latest synthesis experiments conducted in a two-liter reactor for each substrate. For the ion exchange process, catalyst preparation data was taken and upscaled accordingly.

Given the novel nature of these carbonates, market prices are inherently high (Table 1, entries 2, 4, 6). Under current conditions, the cost of the synthesized carbonates is too high, making a straightforward economic analysis impractical. To derive a more realistic pricing model, the selling price for each carbonate was set at 50 €/kg above the cost of its corresponding epoxide precursor. Based on this adjustment, the estimated market prices are as follows: butylene carbonate at 121 €/kg, glycerol carbonate at 328 €/kg, and AGC at 286 €/kg.

5.7.1 Assumptions

- The heating process is assumed to have perfect heat transfer efficiency, with no energy losses or external heat dissipation.
- The system operates under ideal conditions, with negligible energy and material losses.
- Specific heat capacities for the chemicals involved were obtained via property analysis using Aspen software [52].
- Labor costs are excluded from the economic analysis.
- Material costs are based on current market prices.

5.7.2 Ion exchange

The ion exchange process is treated separately from the cyclic carbonate synthesis. In this process, 1.000 kg of ion-exchange catalyst is produced per batch.

Mass balance
Based on the data received from the latest experimental tests on the ion exchange, the most recent process data has been obtained. Using this information, the mass balance was established (Table 9). Each batch produces 1.000 kg of catalyst following a two-step ion exchange and washing procedure.

Table 9: Mass balance first ion exchange.

Process step	Input	Amount (kg)
Ion exchange:	Potassium iodide	9.200
	Water	37.000
	Amberlite IRA-910 catalyst	1.840
Washing of the catalyst:	Water	183.500
	Acetone	46.000
Output:	Amberlite IRA-910 catalyst	1.420
	Liquid waste	275.000

Operational Expenses (Operational Expenses (OPEX))
The operational expenses clearly indicate that the high cost per kilogram of catalyst is primarily driven by the material costs (Table 10). A major factor in this cost is the unoptimized process, in which the iodide liquid is not recycled but discarded after a single use. Additionally, producing just one kilogram of catalyst requires 18 kilograms of potassium iodide. This inefficiency significantly increases expenses, bringing the cost of one kilogram of catalyst to 3640 €. Given these factors, it was decided not to pursue further examination of the ion exchange process, as it appeared too expensive compared to the non-ion-exchanged catalyst, which costs 16 €/kg (Table 1). Instead, for the cyclic carbonate synthesis, the decision was made to purchase the catalyst outright. Although the price for the synthesized catalyst was not found online, the ion-exchanged catalyst price was estimated to be about the same costs of the chloride form Amberlite IRA-910 20 €/kg.

Table 10: Operational costs ion exchange.

Material	Price to produce one kg of catalyst per reactant.
Potassium iodide	3.170
Water	180
Amberlite IRA-910 catalyst	16
Handling liquid waste	230
Acetone	40
Total material costs	3.640

5.7.3 AGC

Mass balance

The mass balance for each batch of the process was established (Table 11). The target annual production is set at approximately 10.000 tons, with the reaction scaled accordingly to achieve this objective. This production target translates to the execution of 788 batches annually, each yielding 12.600 kg of product. Based on data from recent experimental tests conducted in the two-liter reactor, the process demonstrates a conversion and yield of 98% (Table 4, entry 3). The final purity of AGC reached 96%, as no purification steps were integrated into the reaction process.

Table 11: Mass balance per batch AGC carbonate synthesis.

Input	Amount (kg)
AGE	8.910
Water	310
Amberlite IRA-910 catalyst	270
Carbon dioxide	6.180
Output	Amount (kg)
AGC	12.600
Carbon dioxide	2.840

Energy blance

Now that the mass balance has been established, the energy requirements for the production process can be calculated. An energy balance is crucial for evaluating the viability of the process and determining its associated costs. For the energy balance, the energy requirements of the pumps, compressor, and reactor will be outlined (Table 12). The power usage will be expressed in kWh, as this is a batch process, and the value represents the power required to complete one batch of products. More detailed calculations used for this analysis can be found in the appendix 6.

Table 12: Energy balance per batch AGC carbonate synthesis.

Unit	Power usage per batch (kWh)	Annual power (kWh)	Annual costs
Pumps	0.5	390	30
Compressor	130	102.000	7.130
Reactors	380	300.000	21.000

Reactor and equipment sizing

The reactors and equipment have been sized according to the established mass and energy balance. The total capital expenses for the synthesis process amount to 33.7 million euros (Table 13). The sizing of the reactor was performed using the formula outlined in the book *Chemical Engineering Design* by Sinnott and Towler, as referenced in [51]. The detailed formulas and how they were applied can be found in the appendix 10.6, here all the calculations are performed for the reaction sizing of the AGC synthesis. For this process, ten batch reactors, each with a volume of 10 m^3, are utilized.

Table 13: Equipment sizing and costs AGC.

Unit	Size/Capacity	Costs (k€)	Installed costs (million)
Per reactor	18.225 kg	673	2.7
Total reactor		6.731	26.9
Inlet pumps	16 L/s	525	2.1
Outlet pumps	19 L/s	610	2.5
Storage tanks	250 m3	135	0.5
Compressor	381 kW	670	1.7
CAPEX			33.7

Operational Expenses (OPEX)
The operational expenses of the factory are calculated based on the mass and energy balance previously established, along with the material costs. These expenses account for all materials and energy utilized in the process. Additionally, a 20% overhead is included to cover indirect costs essential for maintaining operations. The catalyst recycling was determined by taking the total annual catalyst requirement and dividing it by two, as demonstrated in the previous section (table 4) to maintain catalyst activity effectively. As a result, the total annual operational costs amount to 1.704 million euros for the production of approximately 10.000 tonnes (Table 14).

Table 14: Operational costs annually AGC.

Material	Annual costs (million)
AGE	1.416,8
Water	0,2
Carbon dioxide	0,8
Amberlite IRA-910 catalyst	2.1
Energy costs	0,03
Overhead (20%)	284,0
OPEX	1.704

Return on Investment (ROI)
Lastly, the return on investment (ROI) is calculated. This is determined by dividing the total amount of revenue from the investment by the total amount of capital expenses, which results in the desired return on investment. A high ROI of 2685% is calculated (Table 15). This indicates that the investment for the AGC synthesis would recoup the invested expenses in about two weeks of operating the factory.

Table 15: Performance Metrics AGC.

	Annually (million)
Revenue	2.834
OPEX	1.704
CAPEX	33,7
Profit	904
ROI (%)	2685%

5.7.4 Butylene carbonate

Mass balance
The mass balance for each batch of the process was established (Table 16). The target annual production is set at approximately 10.000 tons, with the reaction scaled accordingly to achieve this objective. This production target translates to the execution of 788 batches annually, each yielding 12.600 kg of product.

Based on data from recent experimental tests conducted in the two-liter reactor, the process demonstrates a conversion and yield of 98% (Table 6, entry 6). The final purity of butylene carbonate reached 96%, as no purification steps were integrated into the reaction process.

Table 16: Mass balance per batch butylene carbonate carbonate synthesis.

Input	Amount (kg)
Butylene oxide	7.700
Water	310
Amberlite IRA-910 catalyst	230
Carbon dioxide	8.540
Output	**Amount (kg)**
Butylene carbonate	12.600
Carbon dioxide	3.950

Energy balance

Now that the mass balance is set up, the energy requirements for the production process can be calculated. An energy balance is important to show the viability of the process and to determine costs. For the energy balance, the pumps, compressor, and reactor energy requirements will be listed (Table 17). The power usage will be listed in kWh, as this is a batch process, and this is the power required to complete one batch of products. As previously mentioned the extensive calculations used for this can be found in Appendix 6.

Table 17: Energy balance per batch butylene carbonate carbonate synthesis.

Unit	Power usage per batch (kWh)	Annual power (kWh)	Annual costs
Pumps	0.5	390	30
Compressor	230	180.000	12.500
Reactors	400	311.000	22.000

Reactor and equipment sizing

The reactors and equipment are sized according to the established mass and energy balance. The total capital expenses for the synthesis amount to 43.8 million (Table 18). The sizing of the reactor was performed using the formula outlined in the book *Chemical Engineering Design* by Sinnott and Towler, as referenced in [51]. The detailed formula can be found in the 10.6. For this process, ten batch reactors, each with a volume of 10 m^3, are utilized.

Table 18: Equipment sizing and costs Butylene carbonate.

Unit	Size/Capacity	Costs (k€)	Installed costs (million)
Per reactor	24980 kg	920	3.7
Total reactor		9.200	36.7
Inlet pumps	16 L/s	525	2.1
Outlet pumps	19 L/s	610	2.5
Storage tanks	250 m3	135	0.5
Compressor	910 kW	800	2.0
CAPEX			43.8

Operational expenses

The operational expenses of the factory are calculated based on the mass and energy balance previously established, along with the material costs. These expenses account for all materials and energy utilized in the process. Additionally, a 20% overhead is included to cover indirect costs essential for maintaining operations.The catalyst recycling was determined by taking the total annual catalyst requirement and dividing it by two, as demonstrated in the previous section (table 6) to maintain catalyst activity effectively. As a result, the total annual operational costs amount to 516 million euros for the production of approximately 10.000 tonnes (Table 19).

Table 19: Operational costs annually butylene carbonate.

Material	Annual costs (million)
Butylene oxide	426,8
Water	0,2
Carbon dioxide	1,3
Amberlite IRA-910 catalyst	1,2
Energy costs	0,03
Overhead (20%)	85.9
OPEX	516

Return on Investment (ROI)
Lastly, the return on investment (ROI) is calculated. This is determined by dividing the total amount of revenue from the investment by the total amount of capital expenses, which results in the desired return on investment. A high Table ROI of 813% is calculated (Table 20), indicating that the investment for the butylene carbonate synthesis would recoup the invested expenses in less than two months of operating the factory.

Table 20: Performance Metrics butylene carbonate.

	Annually (million)
Revenue	960,5
OPEX	516
CAPEX	43,8
Profit	355.9
ROI (%)	813%

5.7.5 Glycerol carbonate

Mass balance
The mass balance for each batch of the process was established (Table 21). The target annual production is set at approximately 10.000 tons, with the reaction scaled accordingly to achieve this objective. This production target translates to the execution of 3.150 batches annually, each yielding 3.200 kg of product. Based on data received from the latest experimental tests at the two-liter reactor, the latest process data shows a conversion and yield of 99% and 91%, respectively (Table 8, entry 3). The final purity of glycerol carbonate reached 91%, as no purification steps were integrated into the reaction process.

Table 21: Mass balance per batch glycerol carbonate carbonate synthesis.

Input	Amount (kg)
Glycidol	2.060
Amberlite IRA-910 catalyst	60
Carbon dioxide	2.230
Output	Amount (kg)
Glycerol carbonate	3.220
Carbon dioxide	1.070

Energy blance

Now that the mass balance is set up, the energy requirements for the production process can be established (Table 22). An energy balance is important to show the viability of the process and to determine costs. For the energy balance the pumps, compressor, and reactor energy requirements will be listed in the Table below. The power usage will be listed in kWh as this is a batch process and this is the power required to complete one batch of products. The more extensive calculations used for this can be found in the appendix 6.

Table 22: Energy balance per batch glycerol carbonate carbonate synthesis.

Unit	Power usage per batch (kWh)	Annual power (kWh)	Annual costs
Pumps	0.5	1.600	110
Compressor	73	230.000	16.000
Reactors	125	400.000	28.000

Reactor and Equipment Sizing

The reactors and equipment are sized based on the established mass and energy balance. The total capital expenses for the synthesis amount to 12.1 million euros (Table 23), which is significantly lower compared to the other two capital costs due to the short reaction time, requiring only two reactors instead of ten to achieve the yearly production of 10.000 tonnes. Reactor sizing is determined using the formula provided in [51] (Sinnott and Towler). For this process, two batch reactors, each with a volume of 10 m^3, are utilized.

Table 23: Equipment sizing and costs glycerol carbonate.

Unit	Size/Capacity	Costs (k€)	Installed costs (million)
Per reactor	33.820 kg	1.235	
Total reactor		2.470	9.9
Inlet pumps	3 L/s	32	0.1
Outlet pumps	4 L/s	36	0.1
Storage tanks	250 m3	135	0.5
Compressor	290 kW	590	1.5
CAPEX			12.1

Operational Expenses (OPEX)

The operational expenses of the factory are calculated based on the mass and energy balance previously established, along with the material costs. These expenses account for all materials and energy utilized in the process. Additionally, a 20% overhead is included to cover indirect costs essential for maintaining operations. The catalyst recycling was determined by taking the total annual catalyst requirement and dividing it by two, as demonstrated in the previous section (table 8) to maintain catalyst activity effectively. As a result, the total annual operational costs amount to 2.052,8 million euros for the production of approximately 10.000 tonnes (Table 24).

Table 24: Operational costs annually glycerol carbonate.

Material	Annual costs (million)
Glycidol	1.707,3
Carbon dioxide	1,3
Amberlite IRA-910 catalyst	2
Energy costs	0,03
Overhead (20%)	342,1
OPEX	2.052,8

Return on Investment (ROI)

Lastly, the return on investment (ROI) is calculated by dividing the total revenue generated from the investment by the total capital expenses. This calculation yields the desired ROI. A high ROI of 8360% is determined (Table 25), indicating that the investment for the glycerol carbonate synthesis would recoup the invested expenses in less than one week of operating the factory.

Table 25: Performance Metrics glycerol carbonate.

	Annually (million)
Revenue	3.325
OPEX	2.052,8
CAPEX	12,1
Profit	1017,6
ROI (%)	8360%

5.7.6 Conclusion

The techno-economic analyses for the three cyclic carbonate processes. Based on AGE, butylene oxide, and glycidol demonstrate significant value addition, as evidenced by the high ROI estimates (2685%, 813%, and 8360%, respectively). Despite the capital expenditures and numerous simplifying assumptions (such as perfect heat transfer and the neglect of labor costs), these preliminary results indicate that the cyclic carbonate synthesis processes have promising potential for scale-up. However due to the lack of the costs being further clarified it is hard to estimate the costs. The basis of the techno-economic analysis is the costs of the chemicals and if they are very high they mostly always result in a process with a very high ROI. Further studies should refine these estimates by incorporating more detailed process dynamics and industrial-scale pricing data. The concern is that the available data for the selected chemicals pertains to a production scale that is still too small, resulting in high costs and significant price discrepancies.

6 Discussion

This project aimed to develop an efficient and economically viable process for synthesizing cyclic carbonates from CO_2 and epoxides, targeting high-value applications in polymer production, solvents, and battery electrolytes. Three epoxides AGE, butylene oxide, and glycidol were chosen based on their bio-based origins and industrial relevance. The process utilized an ion-exchanged Amberlite IRA-910 catalyst, which was optimized to achieve high conversion and selectivity in both small-scale (100 mL) and larger-scale (2 L) batch reactors.

Process optimization involved fine-tuning reaction conditions, such as temperature and reaction time. For AGC and butylene carbonate synthesis, elevating the temperature to 100°C and reducing the reaction time from 18 to 7 hours resulted in near-complete conversion and exceptional selectivity. In contrast, although glycerol carbonate synthesis achieved full conversion in as little as 45 minutes, it was accompanied by selectivity issues and notable catalyst deactivation, emphasizing the need for further process refinement in this pathway.

A techno-economic analysis was conducted by incorporating material costs, energy balances, and reactor sizing. Preliminary estimates indicate that, under ideal operating conditions, the process could realize impressive returns on investment (ROI) exceeding 700%, leading to substantial annual profits. However, these figures are highly sensitive to variations in raw material prices and scale-up parameters, and real-world production costs may differ from theoretical estimates.

Despite the promising economic outlook, challenges remain. A significant obstacle is the deactivation of the catalyst over multiple reaction cycles, particularly evident in the glycerol carbonate synthesis. While the catalyst performed well over the first two cycles, further reuse led to a measurable decline in activity. This highlights the necessity for future research focused on in-depth analysis of catalyst deactivation mechanisms and the development of robust regeneration strategies to ensure long-term process viability.

Additionally, although the analysis is based on favorable market conditions and idealized operational assumptions, an actual industrial implementation may encounter logistical challenges and fluctuations in supplier pricing. Such factors could influence the overall economic performance, suggesting that further studies should incorporate more realistic market dynamics and process integration considerations.

7 Conclusion

In conclusion, this thesis demonstrates that cyclic carbonate synthesis via the cycloaddition of CO_2 to epoxides is both technically and economically promising. The research successfully optimized reaction conditions in small-scale reactors and validated these parameters upon upscaling to 2 L batch system. High conversions and yields were achieved for AGC and butylene carbonate, with nearly complete conversion and yield under optimized conditions. Although glycerol carbonate synthesis showed rapid conversion, issues with selectivity and catalyst deactivation were evident, underscoring the need for further catalyst improvement.

The accompanying techno-economic analysis indicates substantial potential returns, even when considering the high cost of bio-based precursors and simplified operational assumptions. Nevertheless, key challenges such as catalyst stability, raw material expenses, and the translation of laboratory-scale efficiencies to industrial processes must be overcome to realize full-scale production.

Ultimately, the study contributes valuable insights into the development of greener chemical processes by effectively coupling CO_2 utilization with sustainable synthesis methods. It lays a solid foundation for future research aimed at enhancing catalyst durability, optimizing reaction parameters, and refining economic models, thereby advancing the industrial viability of CO_2-derived cyclic carbonates.

8 Recommendation

Based on the findings of this study, the following recommendations are proposed to enhance the industrial viability of cyclic carbonate synthesis:

1. **In-Depth Catalyst Deactivation Studies:** Future work should focus on a comprehensive investigation of catalyst deactivation mechanisms. Advanced characterization techniques, such mass spectrometry and X-ray Photoelectron Spectroscopy (XPS), could be employed to identify the specific deactivating species (e.g., polycarbonate residues) and to monitor changes in the catalyst surface chemistry over multiple reaction cycles.
2. **Development of Catalyst Regeneration Strategies:** To mitigate catalyst deactivation, it is essential to develop robust regeneration protocols. Optimizing washing procedures and exploring alternative catalyst formulations may help restore catalyst activity and prolong its lifespan, thereby enhancing overall process efficiency.
3. **Process Optimization and Scale-Up Studies:** Further experiments should aim to refine reaction parameters (e.g., temperature, pressure, and reaction time) to achieve optimal performance under continuous or batch operation. Detailed pilot-scale studies that incorporate realistic heat and mass transfer dynamics are recommended to validate the laboratory-scale findings.
4. **Economic Analysis under Realistic Conditions:** While the current techno-economic analysis provides encouraging ROI estimates, future studies should incorporate more realistic market dynamics, including fluctuations in raw material prices, energy costs, and industrial operating conditions. A sensitivity analysis could offer insights into the economic robustness of the process.

Overall, the study lays a solid foundation for the further development of sustainable cyclic carbonate production and highlights the potential for significant environmental and economic benefits if the identified challenges are adequately addressed.

9 Acknowledgements

In this paper, artificial intelligence was utilized for language assistance for the writing of the text. The refinement of my own work was done by the utilization of the ChatGPT model: GPT-3.5.

10 Appendix

10.1 Appendix 1: Pictures of the reactors

Figure 7: Parr 2 L batch reactor.

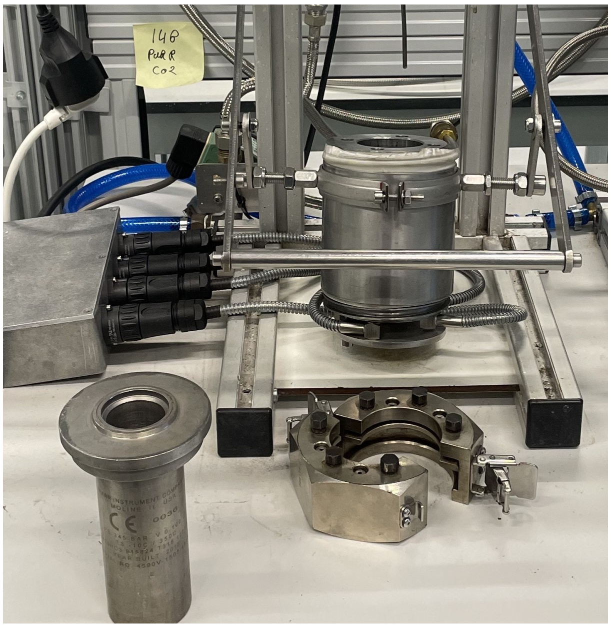

Figure 8: Parr 100 mL batch reactor.

10.2 Appendix 2: ^{1}H NMR of the reaction mixtures

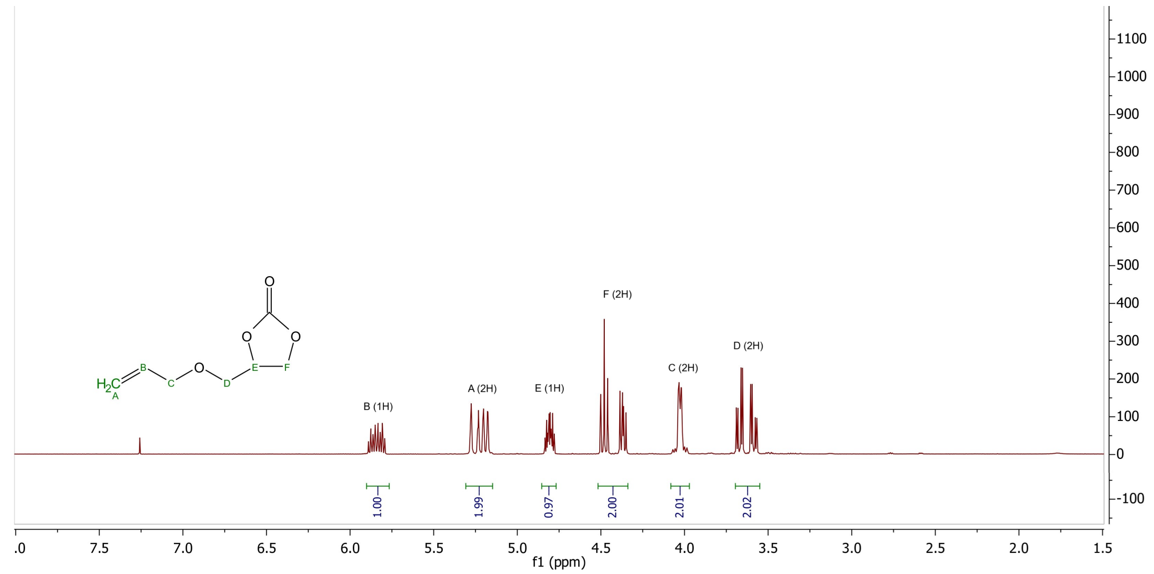

Figure 9: The representative ^{1}H NMR spectrum of the reaction mixture at the end of a catalytic test for the synthesis of allyl glycidyl carbonate (Table 4, entry 2).

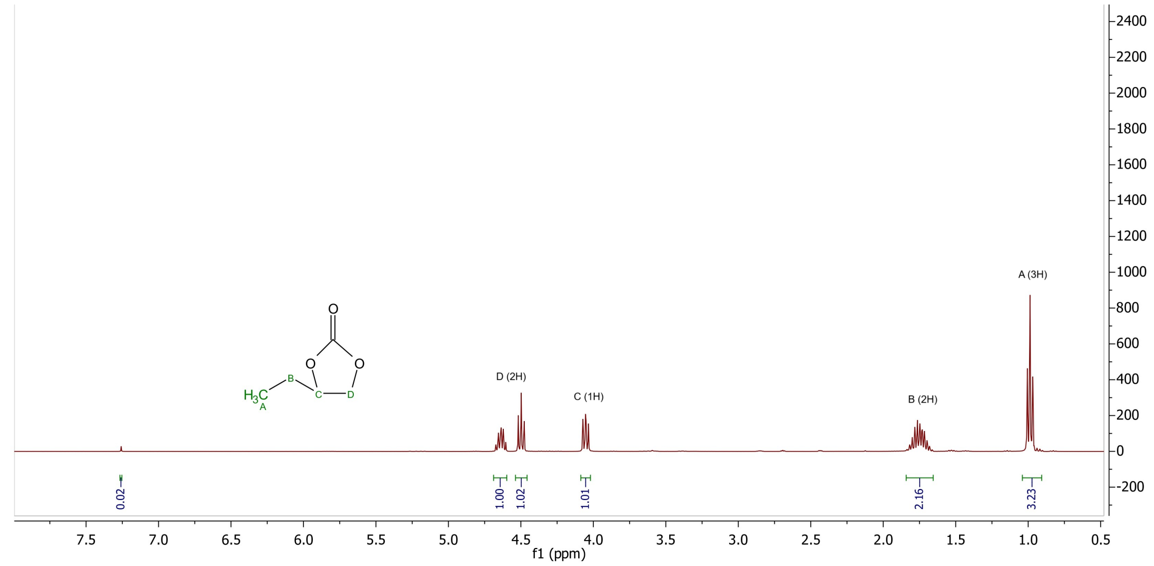

Figure 10: The representative ^{1}H NMR spectrum of the reaction mixture at the end of a catalytic test for the synthesis of butylene carbonate (Table 6, entry 2).

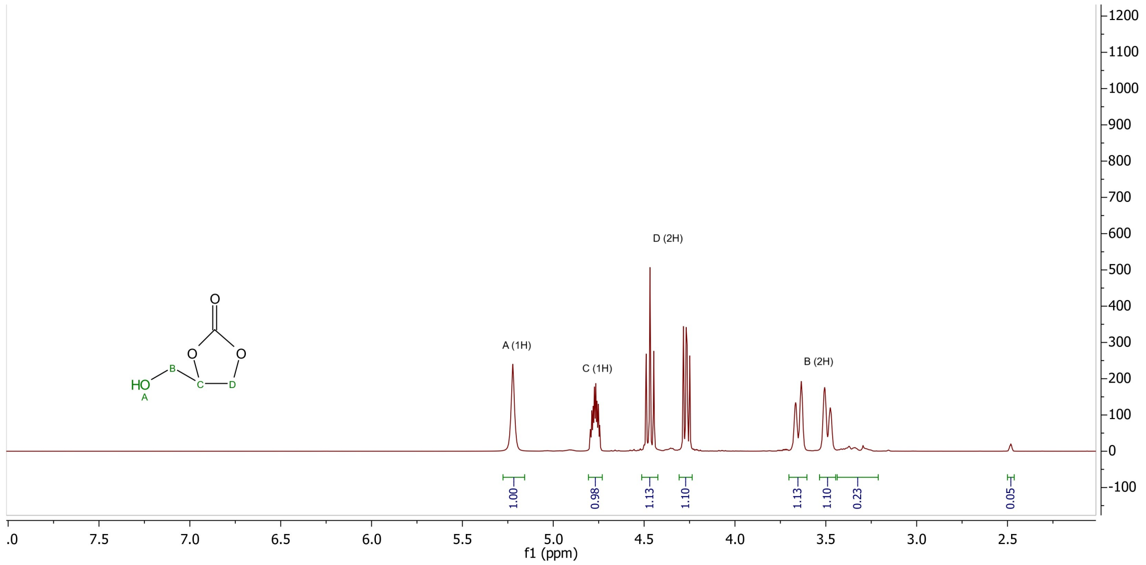

Figure 11: The representative ^{1}H NMR spectrum of the reaction mixture at the end of a catalytic test for the synthesis of glycerol carbonate (Table 7, entry 1).

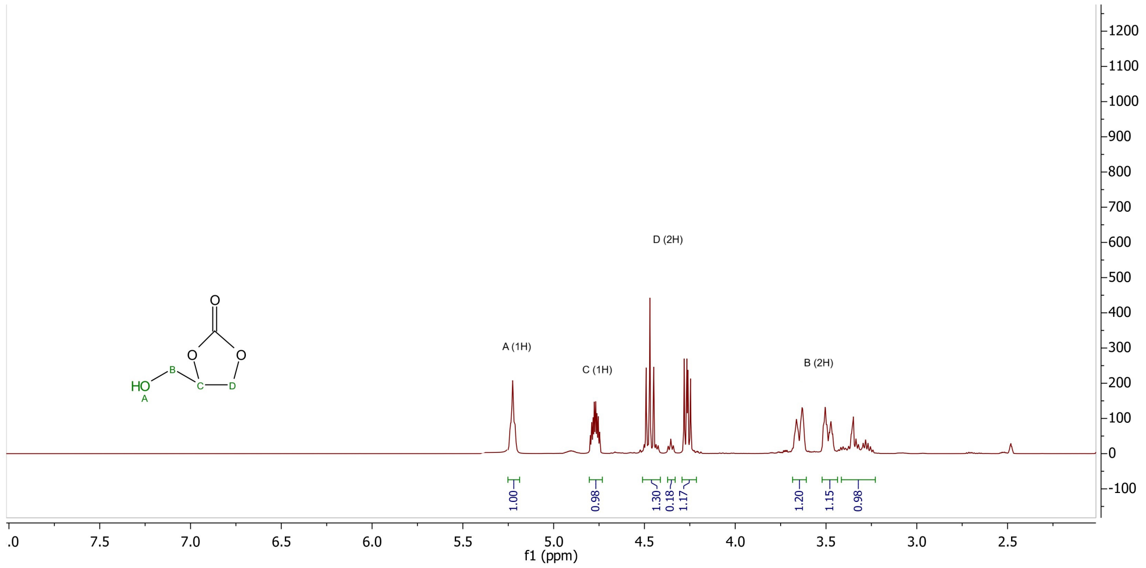

Figure 12: The representative ^{1}H NMR spectrum of the reaction mixture at the end of first recycling test for the synthesis of glycerol carbonate (Table 8, entry 3).

10.3 Appendix 3: Yield and Conversion Calculations Example

For the determination of yield and conversion, the following formula is used:
Epoxide Conversion %:

$$\text{Epoxide Conversion\%} = 100\times\left(1 - \frac{\text{mol of remained epoxide}}{\text{mol of cyclic carbonate} + \text{mol of remained epoxide} + \text{mol of diol, if present}}\right) \tag{4}$$

Cyclic Carbonate Yield %:

$$\text{Cyclic Carbonate Yield\%} = 100\times\left(\frac{\text{mol of product}}{\text{mol of cyclic carbonate} + \text{mol of remained epoxide} + \text{mol of diol, if present}}\right) \tag{5}$$

Cyclic Carbonate Selectivity %:

$$\text{Cyclic Carbonate Selectivity\%} = \left(\frac{\text{Carbonate Yield}}{\text{Epoxide Conversion}}\right) \times 100 \tag{6}$$

These calculations are based on the integrated ^{1}H NMR peaks for the epoxide and carbonate signals. For example, the reaction mixture used to validate butylene carbonate (Table 5, entry 1) was selected because of its clear and distinct peaks (Figure 13). The epoxide conversion was calculated by determining the molar amounts of the remaining epoxide and the produced carbonate, with no dial observed in the mixture Let n_0 be the initial amount of epoxide added (100 mmol). The integrated peak values from the ^{1}H NMR spectrum are given as:

$$I_{\text{epoxide}} = 1.754 \quad \text{and} \quad I_{\text{carbonate}} = 2.346.$$

The total integrated area corresponding to both the epoxide and the carbonate is calculated as:

$$I_{\text{total}} = I_{\text{epoxide}} + I_{\text{carbonate}} = 1.754 + 2.346 = 4.1.$$

The moles of epoxide remaining in the reaction mixture are determined using the ratio of the epoxide integral to the total integral:

$$n_{\text{epoxide, remaining}} = \frac{I_{\text{epoxide}}}{I_{\text{total}}} \times n_0 = \frac{1.754}{4.1} \times 100\,\text{mmol} \approx 42.8\,\text{mmol}.$$

The moles of epoxide that have reacted (converted) are then calculated by subtracting the remaining moles from the initial moles:

$$n_{\text{epoxide, converted}} = n_0 - n_{\text{epoxide, remaining}} = 100\,\text{mmol} - 42.8\,\text{mmol} \approx 57.2\,\text{mmol}.$$

Finally, the percentage conversion of the epoxide is given by:

$$\%\text{Conversion} = \frac{n_{\text{epoxide, converted}}}{n_0} \times 100\% = \frac{57.2\,\text{mmol}}{100\,\text{mmol}} \times 100\% \approx 57\%.$$

Since no other products are present in the mixture, the selectivity toward carbonate formation is nearly 100%. This method doesn't allow quantification of the mass balance. However, no significant side products were detected and no loss of material was observed during the experiment. The ^{1}H NMR data further confirms this, providing additional validation of the accuracy of the calculations.

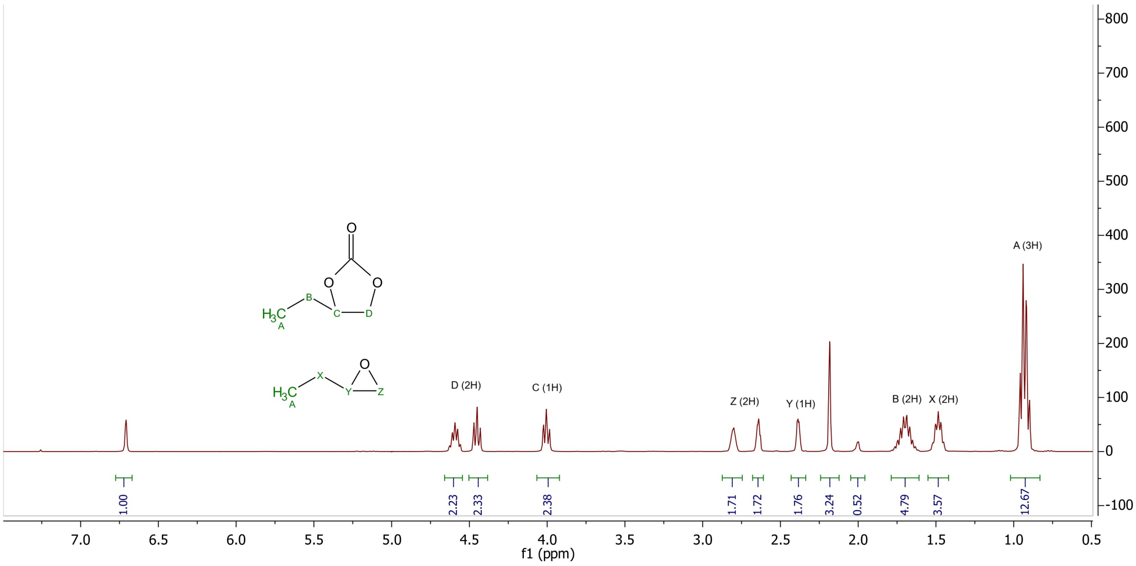

Figure 13: Butylene carbonate ^{1}H NMR (Table 5, entry 1).

10.4 Appendix 4: FT-IR spectra

10.4.1 FT-IR of the Ion exchanged catalyst

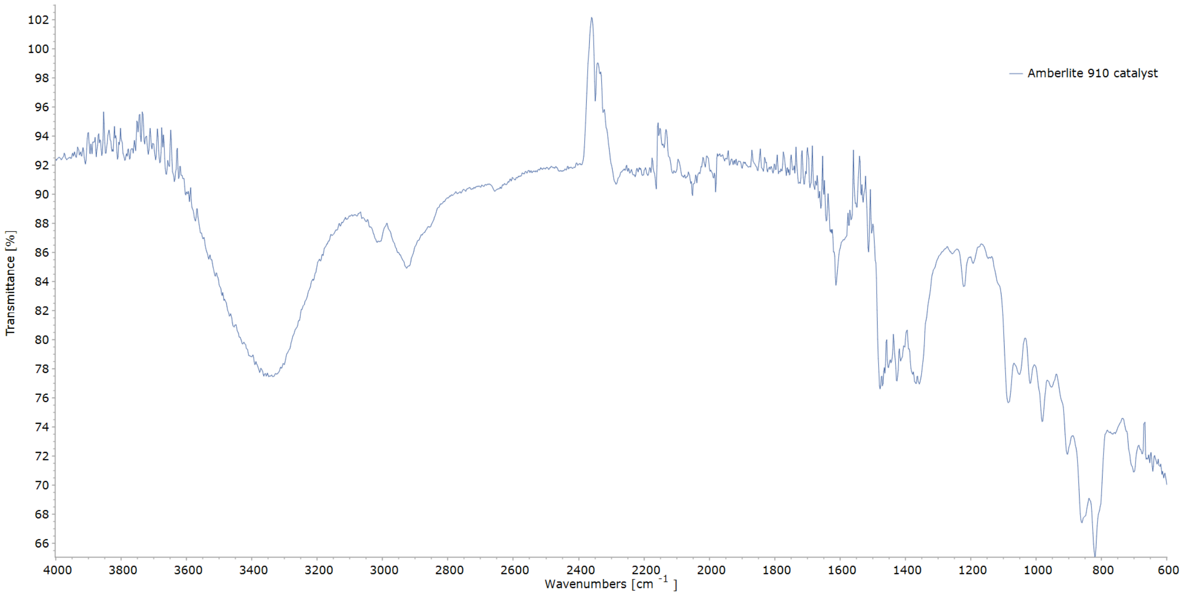

Figure 14: FT-IR Spectra: Ion exchanged catalyst.

10.4.2 FT-IR of the AGC spent catalyst

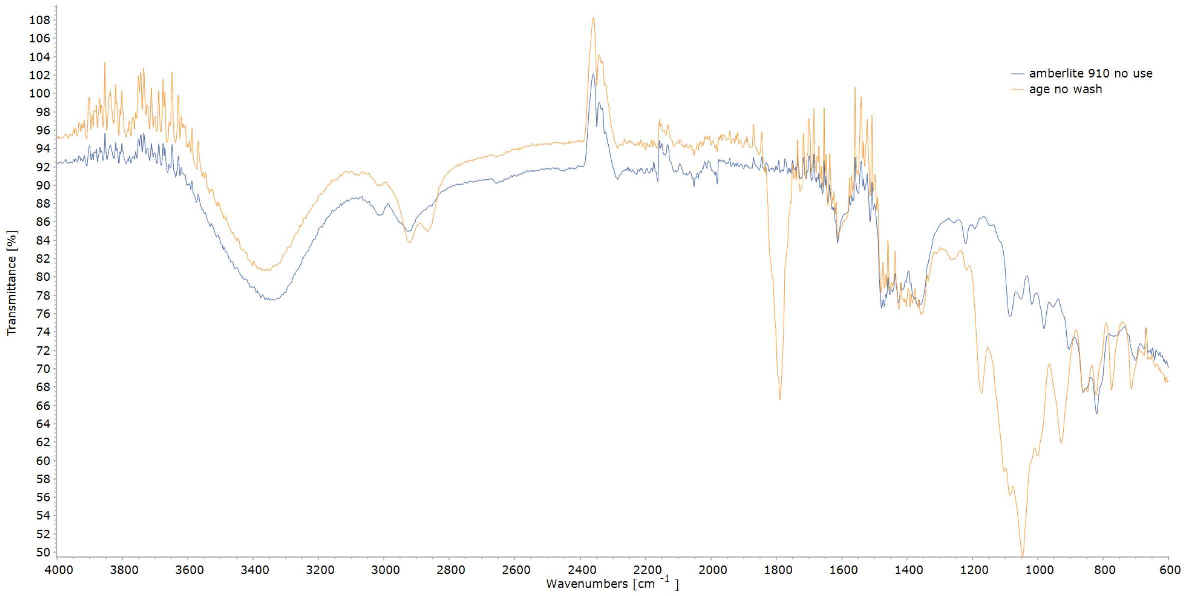

Figure 15: FT-IR Spectra Comparison: Unwashed vs. Ion-Exchanged Catalysts.

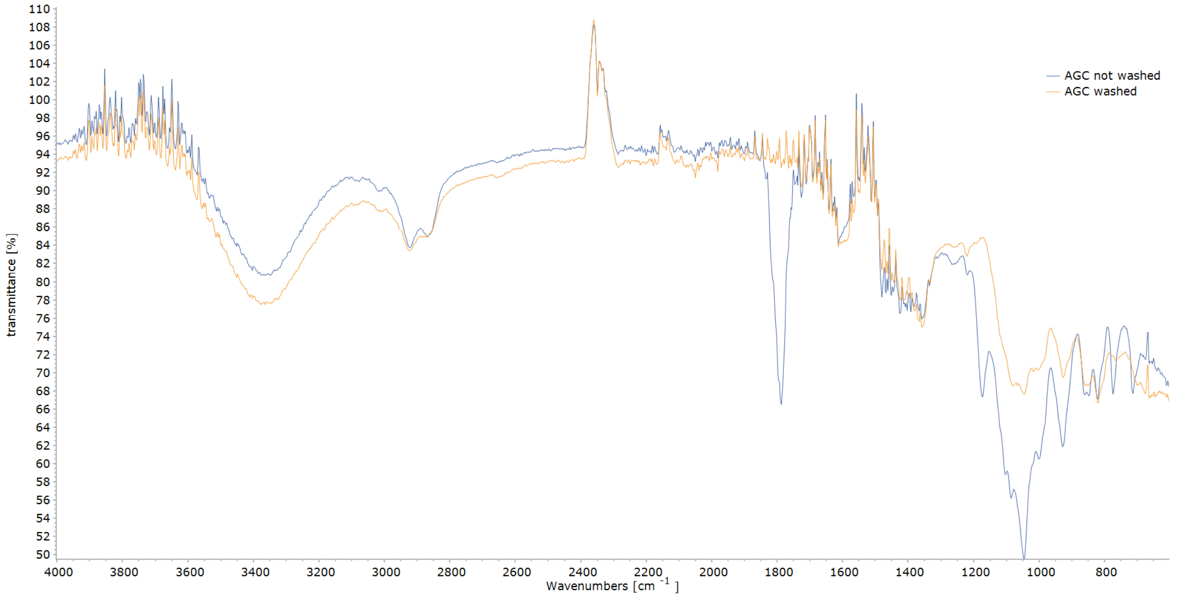

Figure 16: FT-IR Spectra Comparison: Washed vs. Unwashed Catalyst.

10.4.3 FT-IR of the butylene carbonate spent catalyst

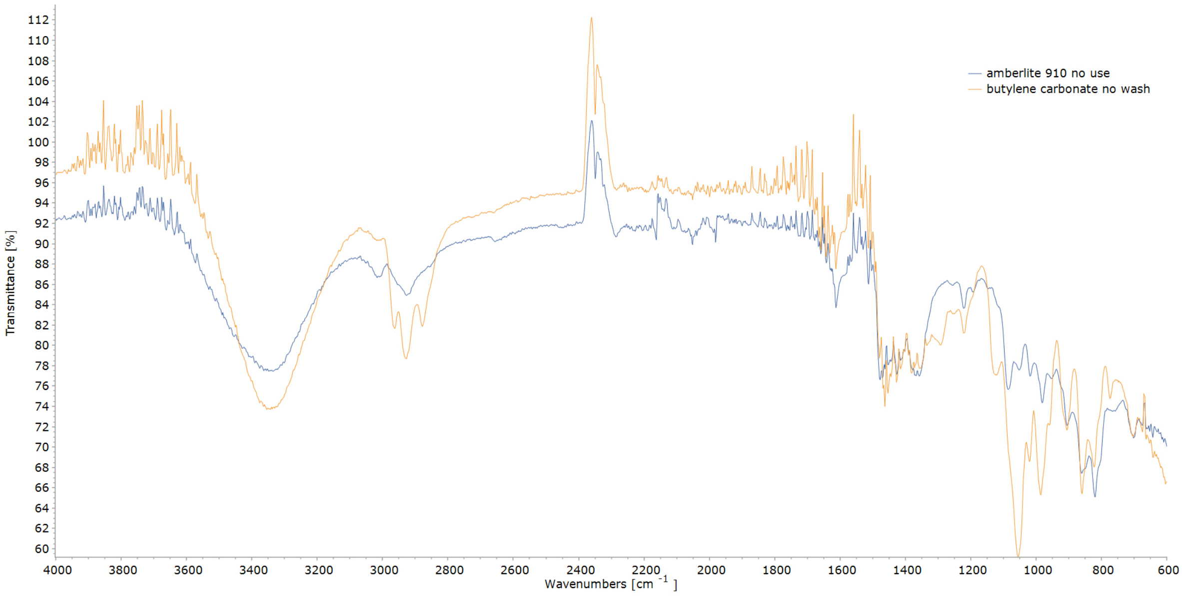

Figure 17: FT-IR Spectra Comparison: Unwashed vs. Ion-Exchanged Catalysts.

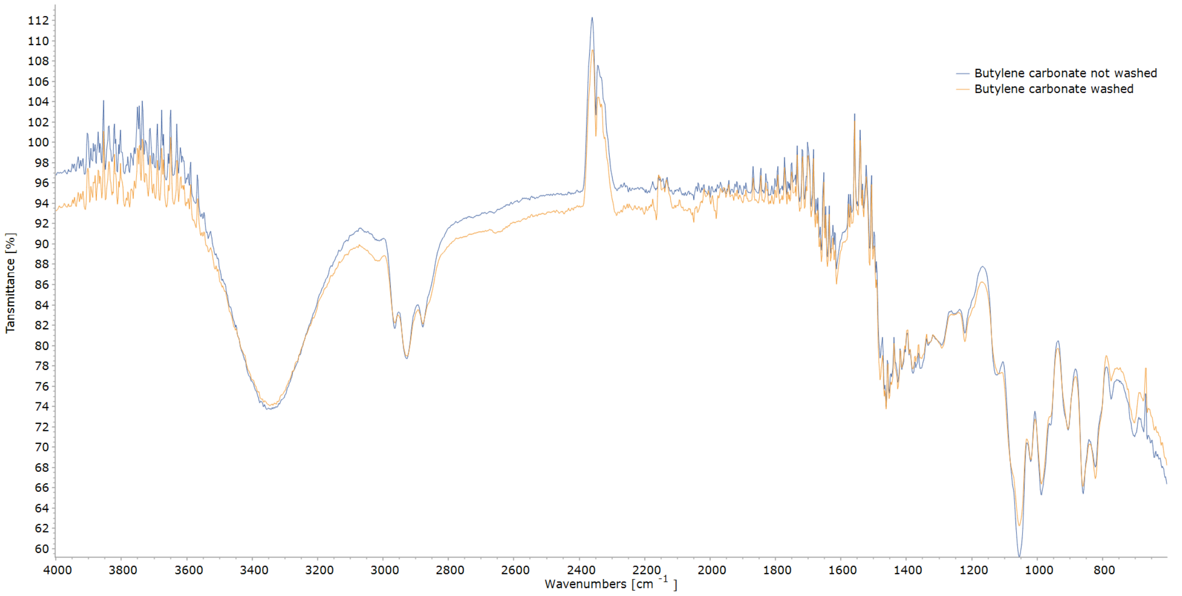

Figure 18: FT-IR Spectra Comparison: Washed vs. Unwashed Catalyst.

10.4.4 FT-IR of the glycerol carbonate spent catalyst

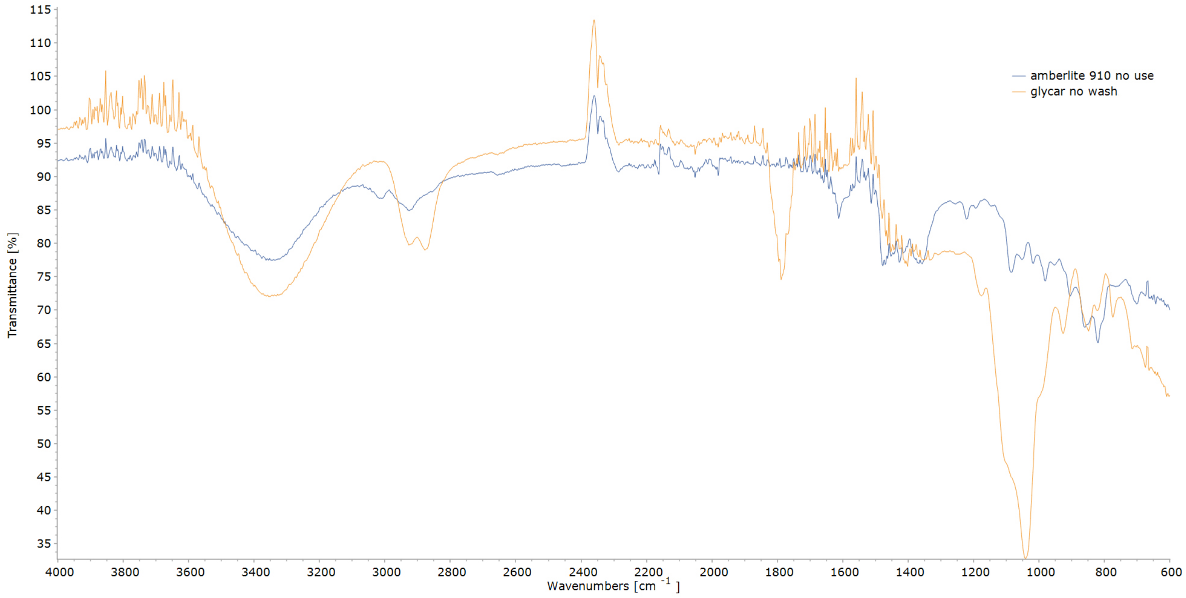

Figure 19: FT-IR Spectra Comparison: Unwashed vs. Ion-Exchanged Catalysts.

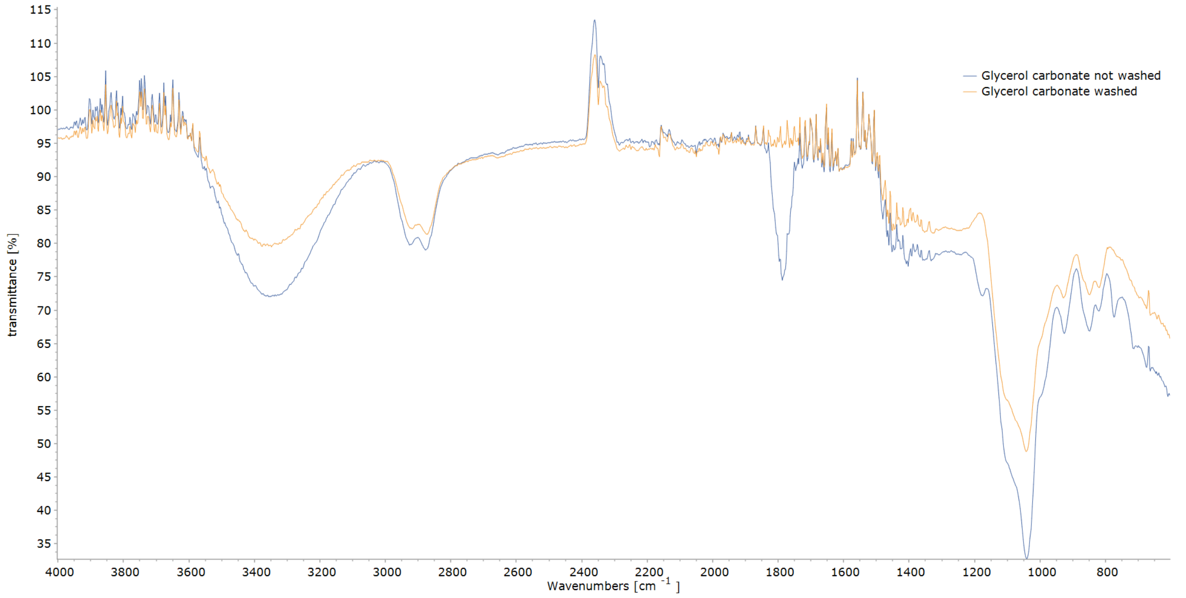

Figure 20: FT-IR Spectra Comparison: Washed vs. Unwashed Catalyst.

10.5 Appendix 5: Pictures of catalysts

Figure 21: Ion exchanged amberlite IRA-910.

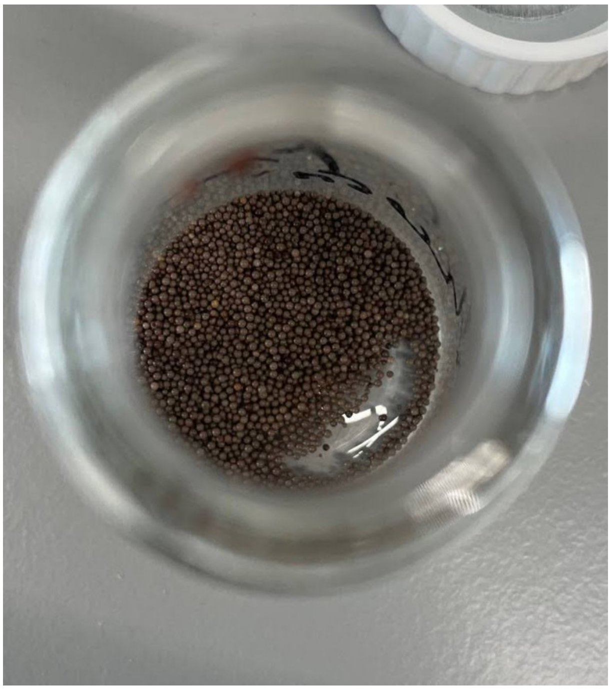

Figure 22: Spent catalyst AGC synthesis not washed.

Figure 23: Spent catalyst AGC synthesis washed.

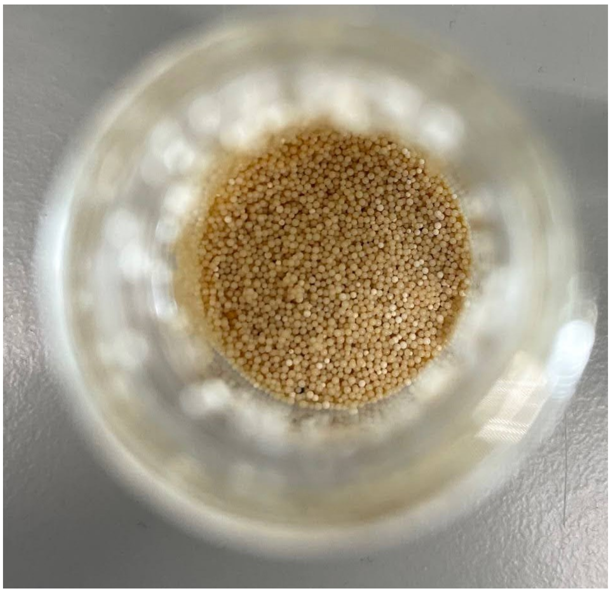

Figure 24: Spent catalyst butylene carbonate synthesis not washed.

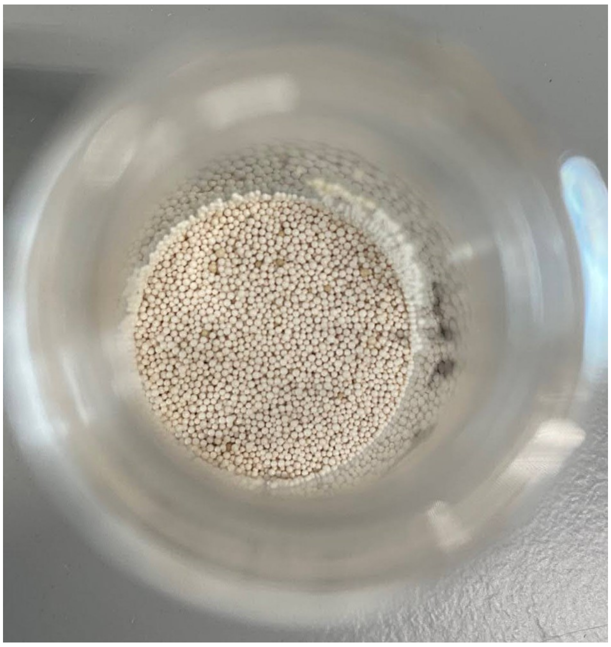

Figure 25: Spent catalyst butylene carbonate synthesis washed.

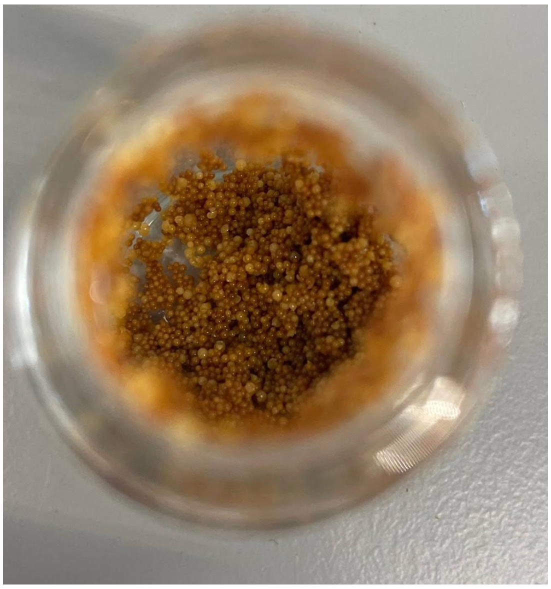

Figure 26: Spent catalyst glycerol carbonate synthesis not washed.

Figure 27: Spent catalyst glycerol carbonate synthesis washed.

10.6 Appendix 6: Calculations for the Techno-Economic Analysis.

The following formulas are used to calculate the sizing and equipment sizing. These formulas are utilized. Example calculations will be given based on the calculations performed for the allyl glycidyl ether synthesis. Firstly, we will go over how the energy required for the process was calculated, followed by the reactor and equipment sizing. All the formulas were obtained from Chemical Engineering Design (SINNOTT and Towler) [51].

Heating of the Reactor

To calculate the energy required per batch of product, the following formula is used:

$$Q = m \cdot c \cdot \Delta T$$

Where:

- Q = Heat energy required for heating (J)
- m = Mass of the reaction mixture (kg)
- c = Specific heat capacity of the mixture (J/kg·°C)
- ΔT = Change in temperature (°C)

Given:

- $m = 9485$ kg
- $c = 1810$ J/kg·°C
- $\Delta T = 80$°C

Substituting:

$$Q = 9485 \cdot 1810 \cdot 80 = 1.373 \times 10^9 \text{ J}$$

Converting to kWh:

$$\frac{1.373 \times 10^9}{3.600 \times 10^6} = 381 \text{ kWh}$$

Thus, the energy required per batch is 381 kWh.

Isentropic Compression of an Ideal Gas

The work required for the compressor is calculated using:

$$W = \frac{RT}{\gamma - 1} \left[\left(\frac{P_2}{P_1} \right)^{\frac{\gamma - 1}{\gamma}} - 1 \right]$$

Where:

- W = Work done (J)
- R = Specific heat capicity (J/kg·K)
- T = Temperature (K)
- γ = Adiabatic index (Cp/Cv)
- P_1 = Initial pressure (bar)

- P_2 = Final pressure (bar)

Given:

- $R = 188.92$ J/kg·K [53]
- $\gamma = 1.298$[53]
- $P_1 = 10$ bar
- $P_2 = 35.88$ bar
- $T = 293$ K

Pump Flowrate Calculation

To determine the flow rate for the pumps, the total amount of fluid is calculated. The inlet and outlet pumps have different flow rates because the outlet stream needs to pump a larger volume. The reactor must be filled and emptied within 10 minutes (600 seconds). The total volume to be filled is 9.49 m^3, and the total volume to be emptied is 11.48 m^3.

$$Q = \frac{V}{t}$$

Substituting the values into the equation results in a total volumetric flowrate of 16 L/s for the inlet pump and 19 L/s for the outlet pump.

Pump Power Calculation

To determine the power required for the pump, we use:

$$P = \frac{Q \cdot \rho \cdot g \cdot H}{\eta}$$

Where:

- P = Power required (W)
- Q = Flow rate (m^3/s)
- ρ = Density of the fluid (kg/m^3)
- H = Pump head (m)
- η = Pump efficiency

Given:

- $Q = 0.066$ m^3/s
- $\rho = 1.1$ kg/m^3
- $g = 9.81$ m^2/s
- $H = 5$ m
- $\eta = 0.7$

Substituting:

$$P = \frac{0.066 \times 1.1 \times 9.81 \times 5}{0.7} = 1.476 \text{ kW}$$

Thickness of Reactor

The minimum reactor wall thickness is given by:

$$t = \frac{d_i \cdot p_i}{(2SE - 1.2p_i)}$$

Where:

- t = Thickness of the shell (m)
- d_i = Internal diameter of the reactor (m)
- S = Maximum allowable pressure inside the reactor (89 N/mm^2)
- p_i = Internal pressure (Pa)
- E = Welding efficiency (assumed 1.0)

Given:

- $d_i = 1$ m
- $S = 89$ N/mm^2
- $p_i = 3,95 * 10^6$ Pa

Substituting:

$$t = \frac{1 \times 39.47}{(2 \times 89 - 1.2 \times 3,95 * 10^6)} = 0.23 \text{ m}$$

Shell Mass Calculation

The shell mass is given by:

$$M = \pi \cdot D_c \cdot \rho \cdot t_w \cdot L_c$$

Given:

- $D_c = 1$ m
- $\rho = 8000$ kg/m^3
- $t_w = 0.23$ m
- $L_c = 3.18$ m

Substituting:

$$M = \pi \times 1 \times 8000 \times 0.23 \times 3.18 = 18.225 \text{ kg}$$

Cost of Equipment/Reactors

The cost of reactors is calculated as:

$$C_e = a + b \cdot S^n$$

Given:

- $a = 15000$

- $b = 68$
- $S = 18.225$
- $n = 0.85$

Substituting:

$$C_e = 15000 + 68 \times 18.225^{0.85} = 673124 \text{ EUR}$$

Installation Factor

To get the final cost, we multiply by the installation factor:

$$I_c = C_e \cdot I_f$$

Given:

- $C_e = 673124$ EUR
- $I_f = 4$

$$I_c = 673124 \times 4 = 2.692.496 \text{ EUR}$$

References

[1] Mette Mikkelsen, Mikkel Jørgensen, and Frederik C Krebs. "The teraton challenge. A review of fixation and transformation of carbon dioxide". In: *Energy & Environmental Science* 3.1 (2010), pp. 43–81.

[2] Paolo P Pescarmona and Masoumeh Taherimehr. "Challenges in the catalytic synthesis of cyclic and polymeric carbonates from epoxides and CO 2". In: *Catalysis Science & Technology* 2.11 (2012), pp. 2169–2187.

[3] Toshiyasu Sakakura, Jun-Chul Choi, and Hiroyuki Yasuda. "Transformation of carbon dioxide". In: *Chemical reviews* 107.6 (2007), pp. 2365–2387.

[4] Michele Aresta, Angela Dibenedetto, and Antonella Angelini. "Catalysis for the valorization of exhaust carbon: from CO2 to chemicals, materials, and fuels. Technological use of CO2". In: *Chemical reviews* 114.3 (2014), pp. 1709–1742.

[5] Toshiyasu Sakakura and Kazufumi Kohno. "The synthesis of organic carbonates from carbon dioxide". In: *Chemical Communications* 11 (2009), pp. 1312–1330.

[6] Michael North, Riccardo Pasquale, and Carl Young. "Synthesis of cyclic carbonates from epoxides and CO 2". In: *Green Chemistry* 12.9 (2010), pp. 1514–1539.

[7] Aeilke J Kamphuis, Francesco Picchioni, and Paolo P Pescarmona. "CO 2-fixation into cyclic and polymeric carbonates: principles and applications". In: *Green chemistry* 21.3 (2019), pp. 406–448.

[8] Vincent Besse et al. "Synthesis and applications of unsaturated cyclocarbonates". In: *Polymer Chemistry* 4.17 (2013), pp. 4545–4561.

[9] Rongchang Luo et al. "New bi-functional zinc catalysts based on robust and easy-to-handle N-chelating ligands for the synthesis of cyclic carbonates from epoxides and CO 2 under mild conditions". In: *Green Chemistry* 16.9 (2014), pp. 4179–4189.

[10] Eser Bingöl and Ahmet Tuncer Erciyes. "Styrenated Oil Synthesis with Cyclic Carbonate Functional Groups on Polystyrene Segment". In: *Polymers* 13.14 (2021), p. 2343.

[11] Naitao Du et al. *Composite Material Prepreg and its Products and Preparation Method.* Chinese Patent CN1927851A. Assignee: Hongfan Composite Material Science & Technology Co., Ltd.; March 14, 2007. 2007. URL: `https://patents.google.com/patent/CN1927851A/en`.

[12] Hongyu Zhou et al. *High-Temperature Resistant Polyimide Composite Material and Preparation Method Thereof.* Chinese Patent CN103333137A. Assignee: Shandong Dongchen Engineering Material Co., Ltd.; October 2, 2013. 2013. URL: `https://patents.google.com/patent/CN103333137A/en`.

[13] Andrea Ghersi and Giovanni Rovera. *Method and System for Processing Biological Samples.* European Patent Application EP3733635A1. Assignee: Roche Diagnostics GmbH; Priority date: 2019-04-03. Oct. 2020. URL: `https://patents.google.com/patent/EP3733635A1/en`.

[14] Alberto Almena and Mariano Martín. "Technoeconomic analysis of the production of epichlorohydrin from glycerol". In: *Industrial & Engineering Chemistry Research* 55.12 (2016), pp. 3226–3238.

[15] Giacomo M Lari et al. "Towards sustainable manufacture of epichlorohydrin from glycerol using hydrotalcite-derived basic oxides". In: *Green Chemistry* 20.1 (2018), pp. 148–159.

[16] Geun-Chang Chung et al. "New cyclic carbonate solvent for lithium ion batteries: trans-2, 3-butylene carbonate". In: *Electrochemistry communications* 1.10 (1999), pp. 493–496.

[17] Chihiro Maeda, Yuki Miyazaki, and Tadashi Ema. "Recent progress in catalytic conversions of carbon dioxide". In: *Catalysis Science & Technology* 4.6 (2014), pp. 1482–1497.

[18] Benjamin Schaffner et al. "Organic carbonates as solvents in synthesis and catalysis". In: *Chemical reviews* 110.8 (2010), pp. 4554–4581.

[19] Beata Kolesinska et al. "Butanol synthesis routes for biofuel production: trends and perspectives". In: *Materials* 12.3 (2019), p. 350.

[20] Qiling Peng et al. "In situ spectroscopic investigations of electrochemical oxygen reduction and evolution reactions in cyclic carbonate electrolyte solutions". In: *The Journal of Physical Chemistry C* 124.29 (2020), pp. 15781–15792.

[21] Mujing Li and Ziwei Zhou. "Technology for 1, 2-Butylene Oxide Production and Market Analysis". In: *Chemical Engineering Transactions* 114 (2024), pp. 613–618.

[22] Mohamad Faizal Ibrahim, Seung Wook Kim, and Suraini Abd-Aziz. "Advanced bioprocessing strategies for biobutanol production from biomass". In: *Renewable and Sustainable Energy Reviews* 91 (2018), pp. 1192–1204.

[23] Mujing Li and Ziwei Zhou. "Technology for 1, 2-Butylene Oxide Production and Market Analysis". In: *Chemical Engineering Transactions* 114 (2024), pp. 613–618.

[24] César AG Quispe, Christian JR Coronado, and João A Carvalho Jr. "Glycerol: Production, consumption, prices, characterization and new trends in combustion". In: *Renewable and sustainable energy reviews* 27 (2013), pp. 475–493.

[25] Matthieu O Sonnati et al. "Glycerol carbonate as a versatile building block for tomorrow: synthesis, reactivity, properties and applications". In: *Green Chemistry* 15.2 (2013), pp. 283–306.

[26] Scott Christy et al. "Recent progress in the synthesis and applications of glycerol carbonate". In: *Current Opinion in Green and Sustainable Chemistry* 14 (2018), pp. 99–107.

[27] Vatcharaporn Aomchad et al. "Recent progress in the catalytic transformation of carbon dioxide into biosourced organic carbonates". In: *Green Chemistry* 23.3 (2021), pp. 1077–1113.

[28] Maryam Salari et al. "Sustainable glycerol carbonate electrolytes for Li-ion supercapacitors: performance evaluation of butyl, benzyl, and ethyl glycerol carbonates". In: *Materials Advances* 2.18 (2021), pp. 6049–6057.

[29] Claire Muzyka et al. "The Catalytic Coupling of CO2 and Glycidol toward Glycerol Carbonate". In: *ACS Catalysis* 14.16 (2024), pp. 12454–12493.

[30] Agnieszka Wróblewska and Anna Fajdek. "Epoxidation of allyl alcohol to glycidol over the microporous TS-1 catalyst". In: *Journal of Hazardous materials* 179.1-3 (2010), pp. 258–265.

[31] Prisco Prete et al. "Glycidol syntheses and valorizations: Boosting the glycerol biorefinery". In: *Current Opinion in Green and Sustainable Chemistry* 35 (2022), p. 100624.

[32] Claire Muzyka et al. "Intensified Continuous Flow Process for the Scalable Production of Bio-Based Glycerol Carbonate". In: *Angewandte Chemie* 136.10 (2024), e202319060.

[33] Mengshuai Liu et al. "Hydrogen bond activation strategy for cyclic carbonates synthesis from epoxides and CO2: current state-of-the art of catalyst development and reaction analysis". In: *Catalysis Reviews* (2019).

[34] Yasser A Alassmy, Zahra Asgar Pour, and Paolo P Pescarmona. "Efficient and easily reusable metal-free heterogeneous catalyst beads for the conversion of CO2 into cyclic carbonates in the presence of water as hydrogen-bond donor". In: *ACS Sustainable Chemistry & Engineering* 8.21 (2020), pp. 7993–8003.

[35] Vatcharaporn Aomchad et al. "Recent progress in the catalytic transformation of carbon dioxide into biosourced organic carbonates". In: *Green Chemistry* 23.3 (2021), pp. 1077–1113.

[36] Statista. *Netherlands: Monthly wholesale electricity price from January 2022 to January 2025.* Accessed: February 2025. 2025. URL: `https://www.statista.com/statistics/1314549/netherlands-monthly-wholesale-electricity-price/`.

[37] Sigma-Aldrich. *Product information for G5809.* Accessed: February 2025. 2025. URL: `https://www.sigmaaldrich.com/NL/en/product/aldrich/g5809`.

[38] Cymit Química. *4-Hydroxymethyl-1,3-dioxolan-2-one (CAS 931-40-8)*. Accessed: February 2025. 2025. URL: `https://cymitquimica.com/products/IN-DA0034YW/931-40-8/4-hydroxymethyl-13-dioxolan-2-one/`.

[39] Sigma-Aldrich. *Product information for A32608*. Accessed: February 2025. 2025. URL: `https://www.sigmaaldrich.com/NL/en/product/aldrich/a32608`.

[40] Chemscene. *Product information for CAS 826-29-9*. Accessed: February 2025. 2025. URL: `https://www.chemscene.com/826-29-9.html`.

[41] Sigma-Aldrich. *Product information for MM/820551*. Accessed: February 2025. 2025. URL: `https://www.sigmaaldrich.com/NL/en/product/mm/820551`.

[42] eChemCloud. *5-Hydroxy-2,2-dimethyl-1,3-dioxane (CAS 4437-85-8)*. Accessed: February 2025. 2025. URL: `https://www.echemcloud.com/search?s=4437-85-8`.

[43] Serv-A-Pure. *Serv-A-Pure IBC BULK 330 Gallon IBC Tote of Deionized Water*. Accessed: February 2025. 2025. URL: `https://www.servapure.com/Serv-A-Pure-IBC-BULK-330-330-Gallon-IBC-Tote-of-Deionized-Water-CONTACT-US-FOR-CUSTOM-SHIPPING-QUOTE_p_10865.html`.

[44] eChemi. *Acetone information page*. Accessed: February 2025. 2025. URL: `https://www.echemi.com/pip/acetone-pid_Rock3929.html`.

[45] Echemi. *Amberlite IRA-910 Product Page*. Accessed: March 2025. 2025. URL: `https://www.echemi.com/produce/pr2404169443-amberlite-ira-910.html`.

[46] Sigma-Aldrich. *Product information for SIGALD/221945*. Accessed: February 2025. 2025. URL: `https://www.sigmaaldrich.com/NL/en/product/sigald/221945`.

[47] Paolo P Pescarmona. "Cyclic carbonates synthesised from CO2: Applications, challenges and recent research trends". In: *Current Opinion in Green and Sustainable Chemistry* 29 (2021), p. 100457.

[48] Chang-Jing Ji, Yu-Jie Hu, and Bao-Jun Tang. "Research on carbon market price mechanism and influencing factors: a literature review". In: *Natural Hazards* 92 (2018), pp. 761–782.

[49] Aastha Dutta. "Fourier transform infrared spectroscopy". In: *Spectroscopic methods for nanomaterials characterization* (2017), pp. 73–93.

[50] George Socrates. *Infrared and Raman Characteristic Group Frequencies: Tables and Charts*. 3rd. Accessed: 2012-12-05. John Wiley & Sons, 2004. ISBN: 978-0-470-09307-8.

[51] Gavin Towler and Ray Sinnott. *Chemical engineering design: principles, practice and economics of plant and process design*. Butterworth-Heinemann, 2021.

[52] Aspen Technology. *Aspen Plus*. `https://www.aspentech.com/en/resources/aspen-plus`. Accessed: 2025-03-02. 2025.

[53] Joseph Hilsenrath. *Tables of thermal properties of gases: comprising tables of thermodynamic and transport properties of air, argon, carbon dioxide, carbon monoxide, hydrogen, nitrogen, oxygen, and steam*. Vol. 564. US Department of Commerce, National Bureau of Standards, 1955.